

Simulating 2+1-flavor QCD on fine lattices with Mobius domain-wall fermions

Shoji Hashimoto (KEK, Sokendai)
@ HHIQCD, YITP, Kyoto University,
Feb 25, 2015

JLQCD collaboration

- Members

- KEK: G. Cossu, B. Fahy, S. Hashimoto, T. Kaneko, H. Matsufuru, J. Noaki, M. Tomii
- Osaka: H. Fukaya, T. Onogi, A. Tomiya
- Kyoto: S. Aoki, T. Iritani
- Tsukuba: Y.G. Cho, Y. Taniguchi
- RIKEN: N. Yamanaka
- Columbia: X. Feng

- Machines @ KEK

- Hitachi SR16000 M1
- IBM Blue Gene /Q



LQCD with chiral fermions

Benefit

- Chiral (or physical quark mass) limit exists at finite lattice spacing.
- χ PT can be applied directly. No extra terms needed in the chiral extrapolation.
- Renormalization simpler, e.g. $Z_V=Z_A$.
- There are sensitive quantities, e.g. chiral condensate, ...
- $U_A(1)$ anomaly manifest.

Loss

- **SLOW:** typically $\times 10 - \times 100$
 - If 100x slower than Wilson, why not reducing lattice spacing by a factor of 2-3 with Wilson? (Not the case!)
- Topology freezing
 - Topological charge is well-defined. Config space is divided into topological sectors with sharp boundaries. HMC hits the boundary.



JLQCD collaboration

2006~2012

- Mid-scale simulations with exactly chiral fermions
 - dynamical overlap fermions: 2, 2+1 flavors
 - single lattice spacing ~ 0.11 fm
 - $16^3 \times 48$, $24^3 \times 48$
- Unique applications
 - ε -regime, Dirac operator spectrum, topological susceptibility
 - VV-AA, strange quark content, $\pi^0 \rightarrow \gamma\gamma$, ...

2012~

- Large-scale simulations with (nearly) chiral fermions
 - Mobius domain-wall fermions: 2+1 flavors
 - multiple lattice spacings ~ 0.08 - 0.04 fm
 - $32^3 \times 64$, $48^3 \times 96$, $64^3 \times 128$
- Applications
 - Main emphasis on heavy quark physics



Details are relevant

- Chiral symmetry breaking = accumulation of near-zero modes.

Banks-Casher relation (1980)

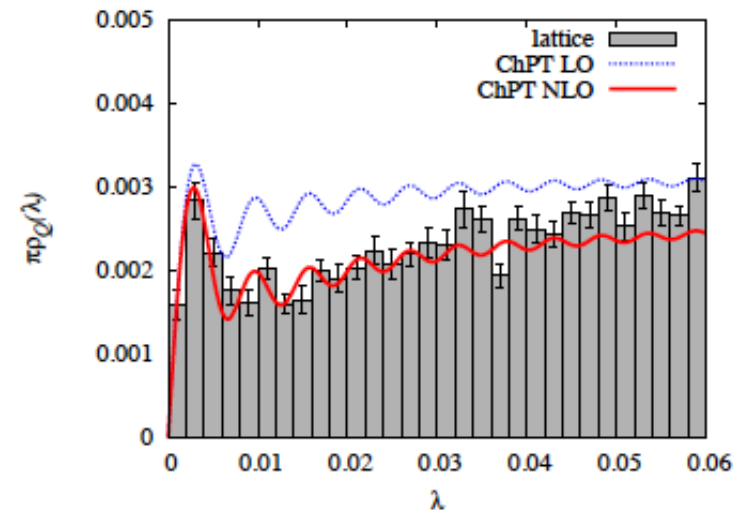
$$-\langle \bar{q}q \rangle = \int_0^\infty d\lambda \rho(\lambda) \frac{2m}{\lambda^2 + m^2} = \pi\rho(0)$$

$\rho(\lambda)$: eigenvalue density

- One can manifestly study the S_χ SB.
- The relevant scale is typically $O(1)$ MeV.

$$\lambda \sim \frac{1}{\Sigma V}$$

JLQCD (2009)



2+1-flavor QCD simulation
with overlap fermions:
exact chiral symmetry.



Plan of this talk

Project and its status:

1. Mobius domain-wall fermion
 - Formulation, residual mass
2. Large-scale simulations
 - Parameters, topology, scale setting
3. First physics results
 - Short-distance current correlators
 - Decay constants (and form factor)



1. Mobius domain-wall fermion

Formulation, residual mass



Chiral symmetry on the lattice

- Lattice fermion action is symmetric under the modified chiral transformation

$$\delta\bar{\psi} = i\alpha\bar{\psi}\left(1 - \frac{D}{2M_0}\right)\gamma_5, \quad \delta\psi = i\alpha\gamma_5\left(1 - \frac{D}{2M_0}\right)\psi$$

if the Dirac operator D satisfies

$$D\gamma_5 + \gamma_5 D = \frac{1}{M_0} D\gamma_5 D \quad \text{Ginsparg-Wilson relation}$$

- Implementation:
 - Domain-wall fermion (Kaplan, Shamir, 1993)
 - Overlap fermion (Neuberger, Narayanan, 1998)

Now, understood to be essentially the same.



Dirac operator

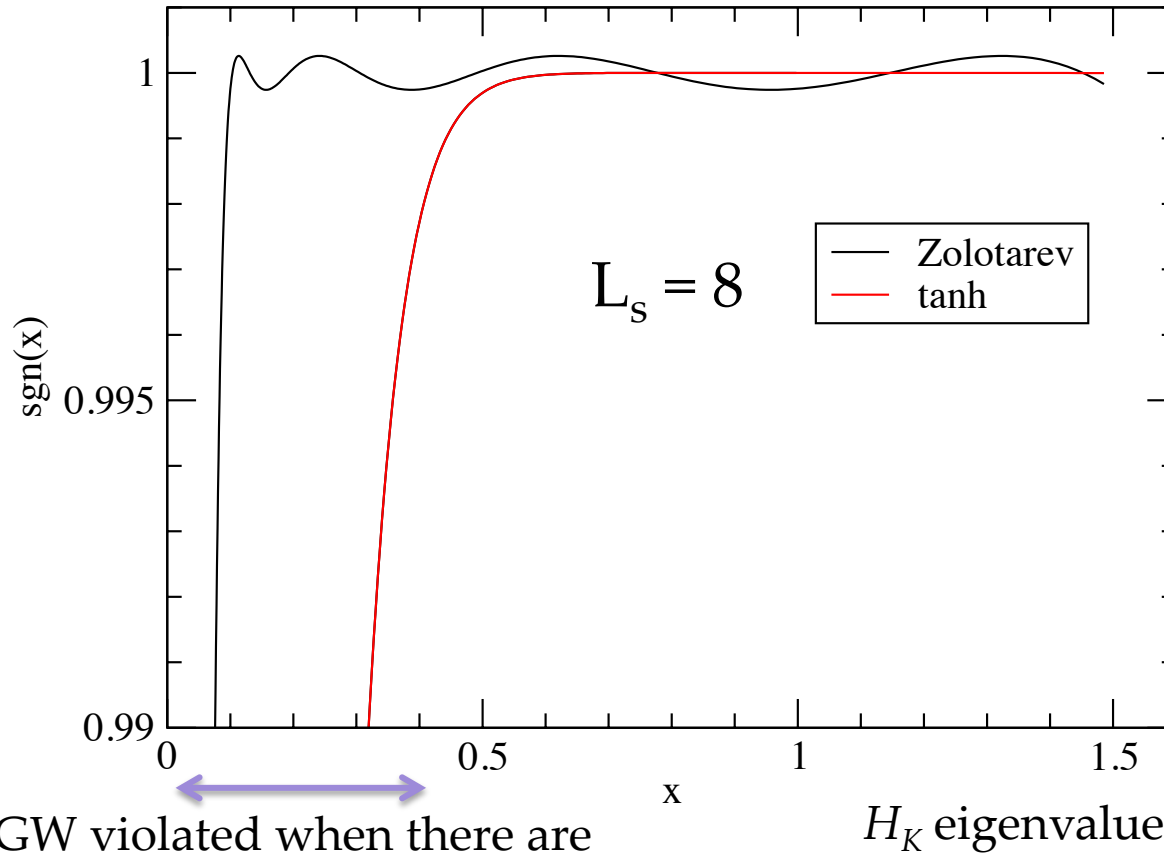
- Effective 4D operator

$$D = \frac{M_0}{a} [1 - \gamma_5 \operatorname{sgn}(aH_K)], \quad H_K = \gamma_5 (D_K - M_0)$$

- written using a matrix sign function “sgn” of the hermitian operator H_K .
 - Common choices: Rational approximation (Zolotarev) or Tanh.
 - Leading disc effect $\sim O(a^2)$, after a trivial field redefinition.
- Kernel operator H_K
 - Borici (or overlap) $H_K = \gamma_5 (D_W - M_0)$
 - Shamir (or domain-wall) $H_K = \gamma_5 (D_W - M_0) / (2 + (D_W - M_0))$



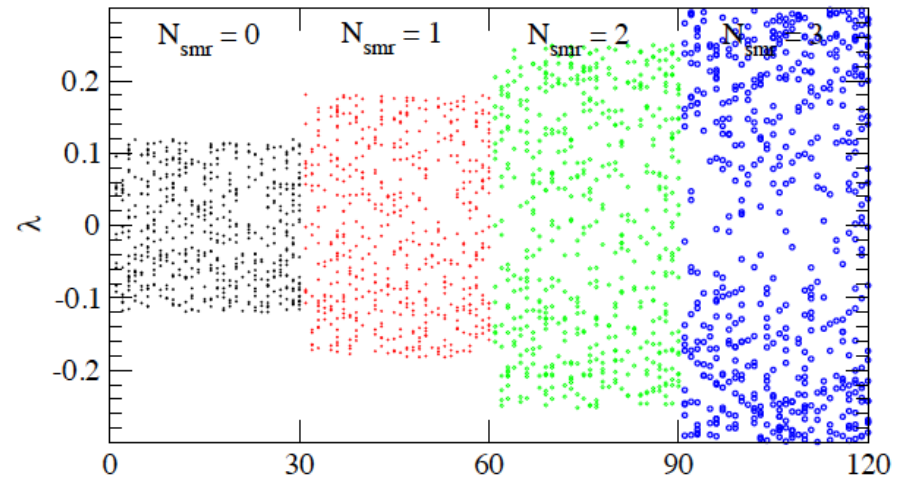
Sign function approximation



Eigenvalue distribution

- Near-zero eigenvalues from rough configs
 - on the topology boundary
 - measure with smeared links
 - stout, $N_{\text{smr}}=0,1,2,3$
- Exact? or good enough?
 - Low-modes are separately treated for *overlap* fermions to ensure exact GW relation.
 - Allow small violation for *domain-wall* fermions. Smeared link improves GW a lot.

$a \sim 0.08$ fm, low-lying ev of H_W



Larger N_{smr} is better, if there is no side-effects.



Generalized 5d implementation

$$S_{GDW} = \sum_x \bar{\psi} D_{GDW}^5 \psi$$

Edwards-Heller (2000)

Chiu (2003): s-dependence introduced

$$D_{GDW}^5 \equiv \begin{pmatrix} (D_-^1)^{-1} D_+^1 & -P_- & 0 & \dots & 0 & mP_+ \\ -P_+ & (D_-^2)^{-1} D_+^2 & -P_- & 0 & \dots & 0 \\ 0 & -P_+ & (D_-^3)^{-1} D_+^3 & -P_- & \ddots & \vdots \\ \vdots & 0 & \ddots & \ddots & \ddots & \vdots \\ 0 & \dots & \ddots & -P_+ & (D_-^{L_s-1})^{-1} D_+^{L_s-1} & -P_- \\ mP_- & 0 & \dots & 0 & -P_+ & (D_-^{L_s})^{-1} D_+^{L_s} \end{pmatrix}$$

$$D_+^s = 1 + b_s D_W(-M_0), D_-^s = 1 - c_s D_W(-M_0); \quad P_{\pm} = (1 \pm \gamma_5) / 2$$

- May reduce to various combinations of kernel/approx
- But, b_s, c_s may depend on s .



Generalized 5d implementation

$$S_{GDW} = \sum_x \bar{\chi} D_\chi^5 \chi$$

- After an unitary transformation,

$$D_\chi^5 \equiv \left(\begin{array}{c|cccccc} P_- - mP_+ & -T_1^{-1} & 0 & \dots & \dots & 0 \\ \hline 0 & 1 & T_2^{-1} & 0 & \dots & 0 \\ \vdots & 0 & 1 & T_3^{-1} & 0 & 0 \\ \vdots & \ddots & \ddots & \ddots & \ddots & \vdots \\ 0 & \dots & \dots & 0 & 1 & T_{L_s-1}^{-1} \\ -T_{L_s}^{-1}(P_+ - mP_-) & 0 & \dots & \dots & 0 & 1 \end{array} \right)$$

$$T_s^{-1} \equiv -(Q_-^s)^{-1} Q_+^{-1}, \quad Q_\pm^s = (D_-^s)^{-1} D_+^s P_\mp - P_\pm$$

- Then, Schur complement

$$\begin{pmatrix} D & C \\ B & A \end{pmatrix} = \begin{pmatrix} 1 & CA^{-1} \\ 0 & 1 \end{pmatrix} \begin{pmatrix} D - CA^{-1}B (\equiv S_\chi) & 0 \\ 0 & A \end{pmatrix} \begin{pmatrix} 1 & 0 \\ A^{-1}B & 1 \end{pmatrix}$$

Note: $\det A = 1$



4D effective operator

- $\det A = 1$ doesn't contribute to path integ.

$$S_\chi(m) = -(1 + T_1^{-1}T_2^{-1}\cdots T_{L_s}^{-1})\gamma_5 \left[\frac{1+m}{2} - \frac{1-m}{2} \gamma_5 \frac{T_1^{-1}T_2^{-1}\cdots T_{L_s}^{-1} - 1}{T_1^{-1}T_2^{-1}\cdots T_{L_s}^{-1} + 1} \right]$$

- Combining with Pauli-Villars ($m=1$), one obtains the 4D effective operator.

$$D^{(4)} \equiv S_\chi^{-1}(m=1)S_\chi(m) = \frac{1+m}{2} - \frac{1-m}{2} \gamma_5 \frac{T_1^{-1}T_2^{-1}\cdots T_{L_s}^{-1} - 1}{T_1^{-1}T_2^{-1}\cdots T_{L_s}^{-1} + 1}$$



approximate the
sign function



Kernels and approximations

- By setting b_s, c_s , one can
 - choose the kernel

$$b_s + c_s \equiv (b + c)\omega_s$$

$$b_s - c_s = b - c$$

$$T_s^{-1} = \frac{1 + \omega_s H_K}{1 - \omega_s H_K}, \quad H_K = \gamma_5 \frac{(b + c)D_W}{2 + (b - c)D_W}$$

Borici (H_W): $b+c=2, b-c=0$
 Shamir (H_T): $b+c=1, b-c=1$

- choose the approximation

- Tanh or Polar decomposition: (domain-wall)

$$\omega_s = 1 \Rightarrow \text{sgn}_{\tanh}(H_T) = \frac{(1 + H_T)^{L_s} - (1 - H_T)^{L_s}}{(1 + H_T)^{L_s} + (1 - H_T)^{L_s}} = \tanh(L_s \tanh^{-1}(H_T))$$

- Zolotarev (rational function, conventional overlap)

$$\text{sgn}_{\text{rat}}[H] = x \left(p_0 + \sum_{l=1}^{N_{\text{pole}}} \frac{p_l}{H^2 + q_l} \right)$$

Optimal Domain-wall (Chiu, 2003)
 = H_W + Zolo



Mobius domain-wall

Brower, Neff, Orginos (2004)

- Favorable choice

$$T_s^{-1} = \frac{1 + H_K}{1 - H_K}, \quad H_K = \gamma_5 \frac{\alpha D_W}{2 + D_W}$$

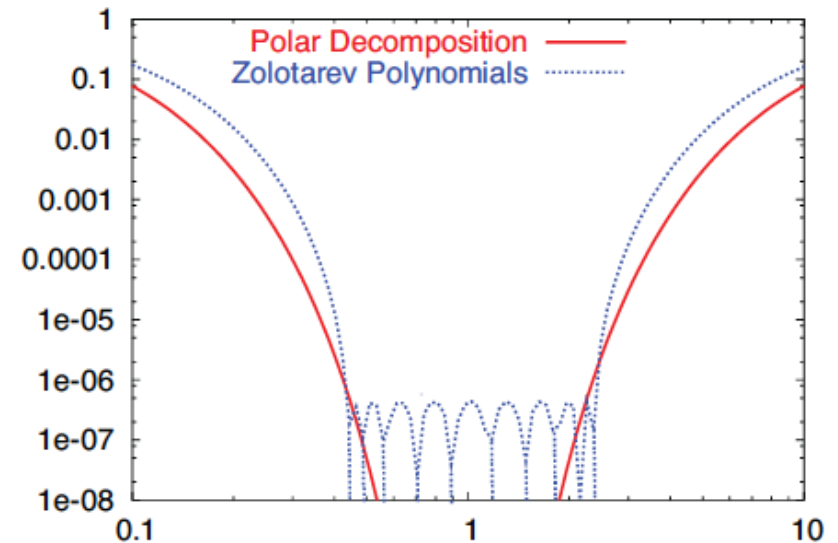
Put a scale factor α on the domain-wall kernel.

- Uses the symmetry property of the polar decomposition

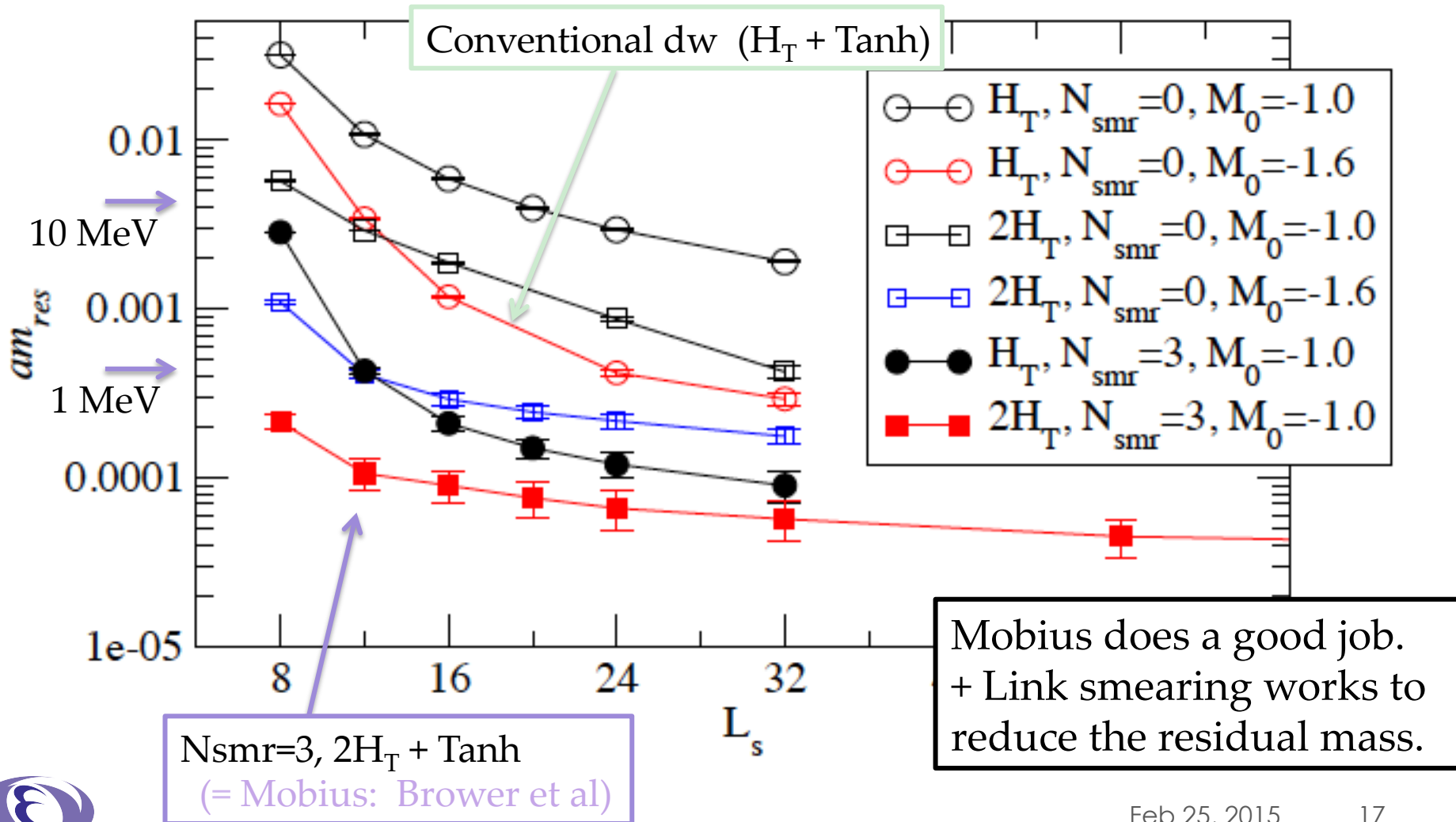
$$\lambda \Leftrightarrow 1/\lambda$$

- Adjust the scale so that the best approximation range is used.

from Brower et al (2012)

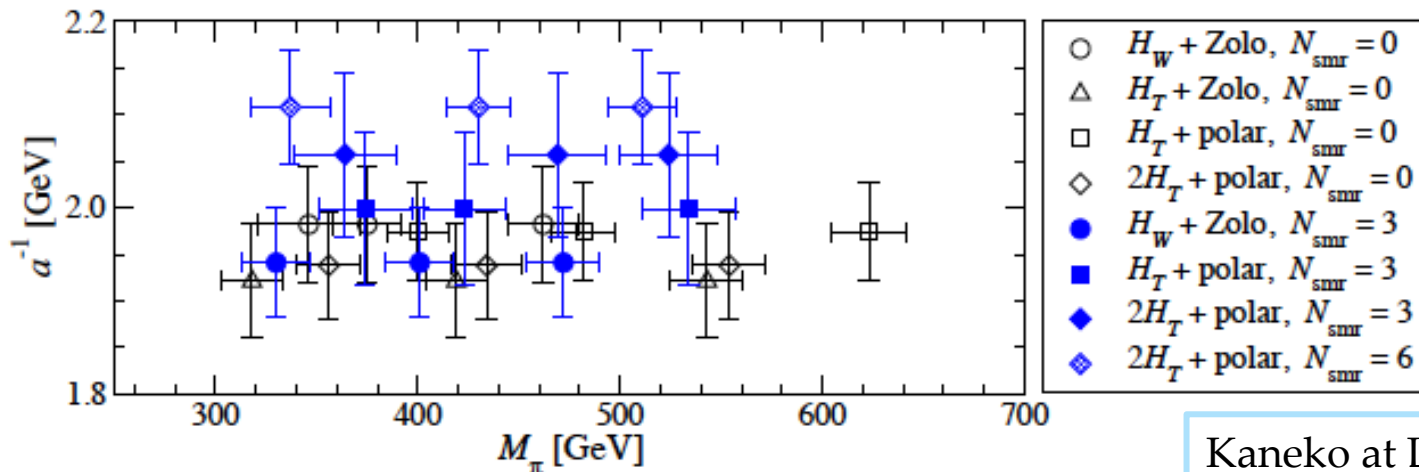


Various choices



Chiral symmetry vs. Cost

- Extensive survey of different kernels and approx., to compare their numerical costs and the violation of chiral symmetry.
 - tree-level Symanzik gauge + $N_f=2$ 5d fermions
 - $16^3 \times 32 \times 12$, $1/a \sim 2$ GeV, $m_\pi=300-600$ MeV
 - $\tau=1$, N_{MD} chosen to achieve 70-90% acc, 1,000 traj each

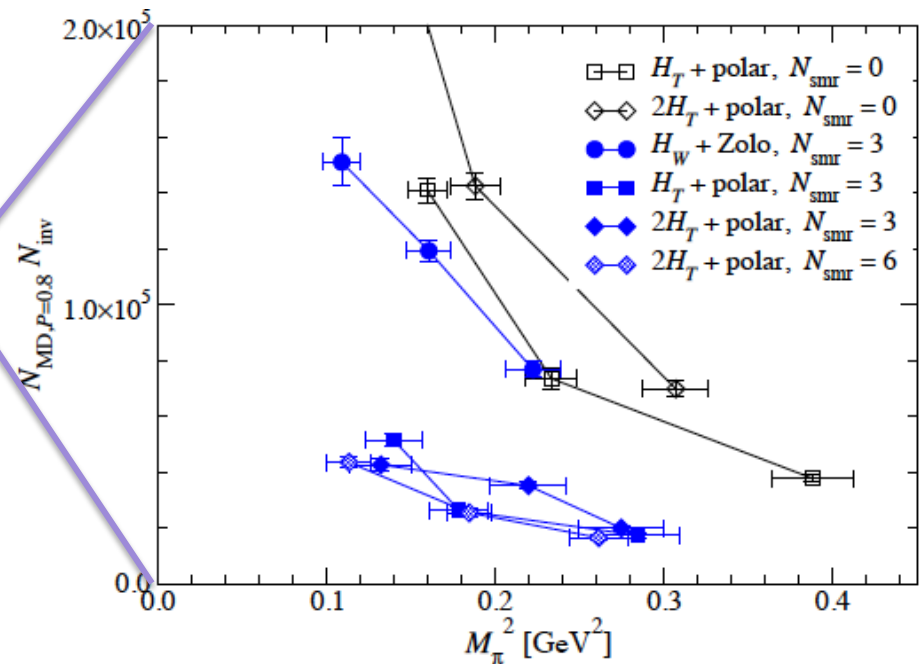
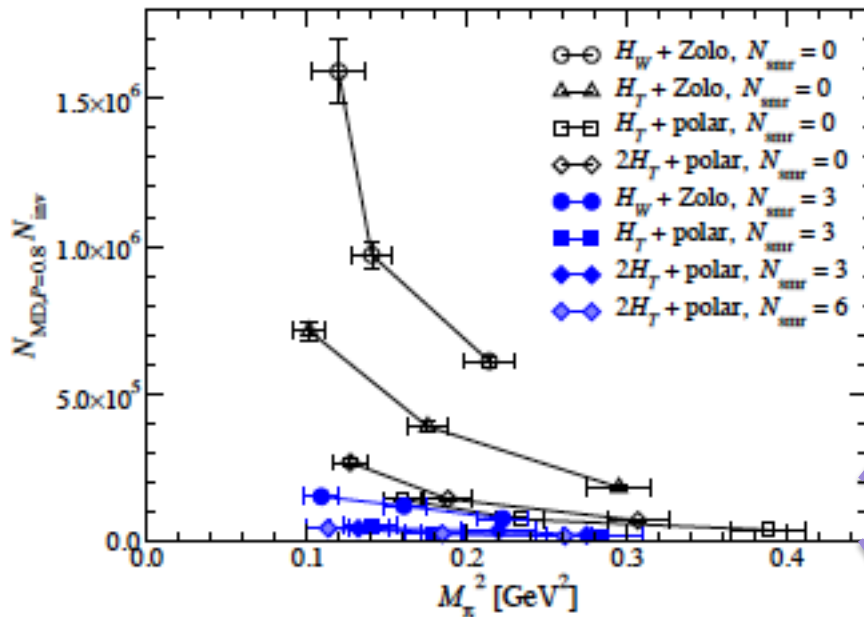


Kaneko at Lattice 2013



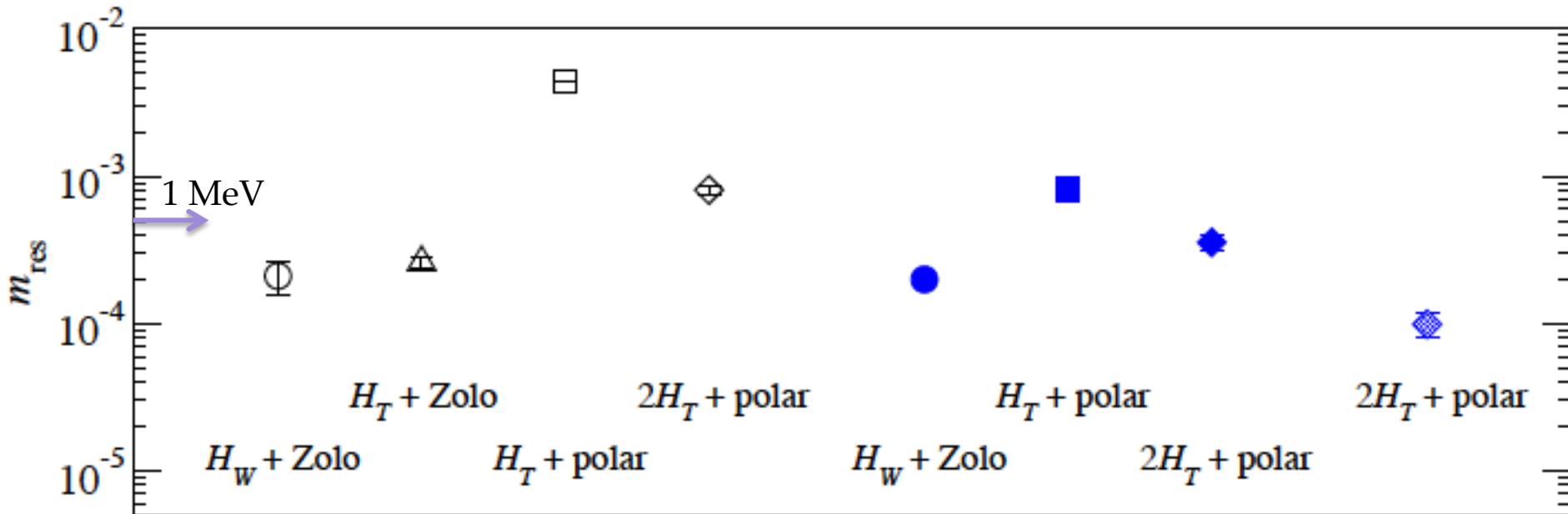
Cost for HMC simulation

- $H_W + \text{Zolo} \rightarrow (2)H_T + \text{polar}$
= x6 speedup
- link smearing
= x(3 or 4) speedup



Residual mass

- A measure of the violation of GW.
 - With a fixed $L_s (=12)$.



With “Zolo” or “ $2H_T + \text{polar}$ ” (or tanh), m_{res} is sufficiently small.



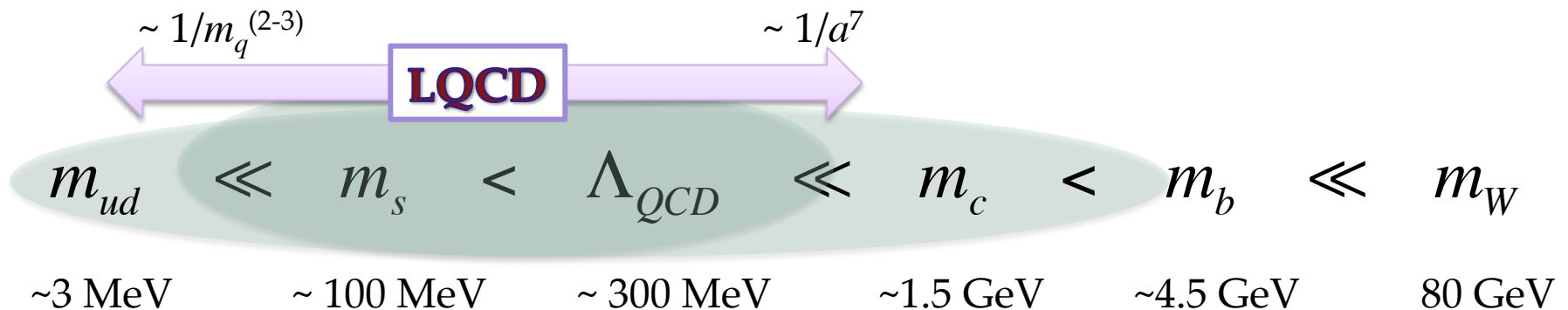
2. Large-scale simulations

Parameters, topology, scale setting



Multi-scale problem

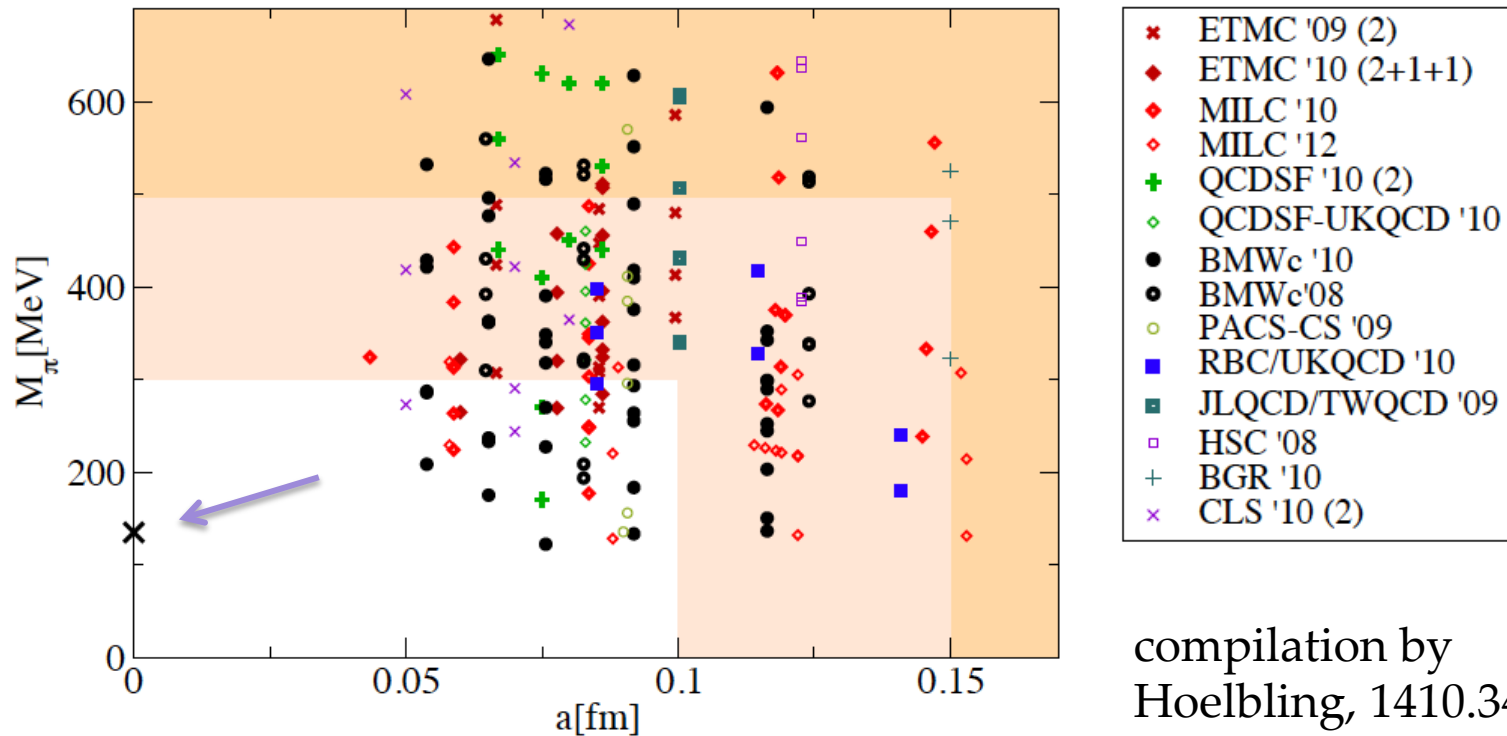
- Players of QCD live between 3 MeV and 5 GeV
 - Not feasible (for now) to treat at once.
(Including nuclear physics, one needs to resolve 1 MeV.)



- Two directions (or both)
 - ← Going to the physical up/down quark masses
 - Fine lattices to directly treat charm (or even bottom)

Recent LQCD simulations

- Approaching the continuum/physical limit



compilation by
Hoelbling, 1410.3403



New simulations of JLQCD

- A new set of ensembles with Mobius domain-wall fermion has been generated (2012~).
 - **Fine lattices:** the lattice spacing in the range $a = 0.043 \sim 0.083$ fm.
 - **Chiral symmetry:** very well satisfied. Residual mass is a few MeV or less, negligible for most applications. For instance, $Z_V = Z_A$ to a good precision.
 - **Topology changes:** Unlike overlap, it moves. But, approaching the continuum limit, long autocorrelation becomes a problem as with other fermion formulations.
 - **Faster than overlap (x20):** With the smeared-link, faster than the conventional domain-wall (x4), while making chiral symmetry better.



Lattice parameters

$\beta = 4.17, 1/a \sim 2.4 \text{ GeV}, 32^3 \times 64 \text{ (x12)}$

m_{ud}	m_π [MeV]	MD time
$m_s = 0.030$		
0.007	310	10,000
0.012	410	10,000
0.019	510	10,000
$m_s = 0.040$		
0.0035	230	10,000
0.0035 ($48^3 \times 96$)	230	10,000
0.007	320	10,000
0.012	410	10,000
0.019	510	10,000

$\beta = 4.35, 1/a \sim 3.6 \text{ GeV}, 48^3 \times 96 \text{ (x8)}$

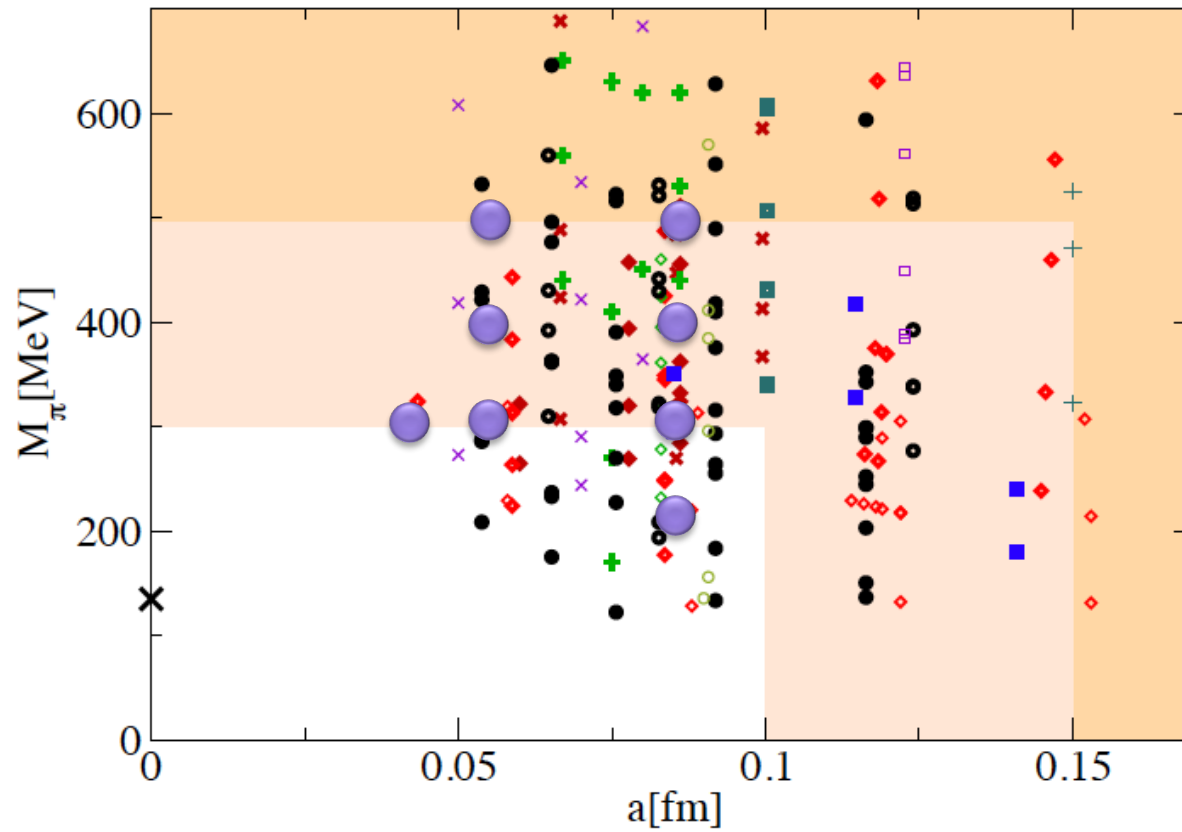
m_{ud}	m_π [MeV]	MD time
$m_s = 0.018$		
0.0042	300	10,000
0.0080	410	10,000
0.0120	500	10,000
$m_s = 0.025$		
0.0042	300	10,000
0.080	410	10,000
0.0120	510	10,000

$\beta = 4.47, 1/a \sim 4.6 \text{ GeV}, 64^3 \times 128 \text{ (x8)}$

0.0030	~ 300	10,000
--------	------------	--------



New ensembles

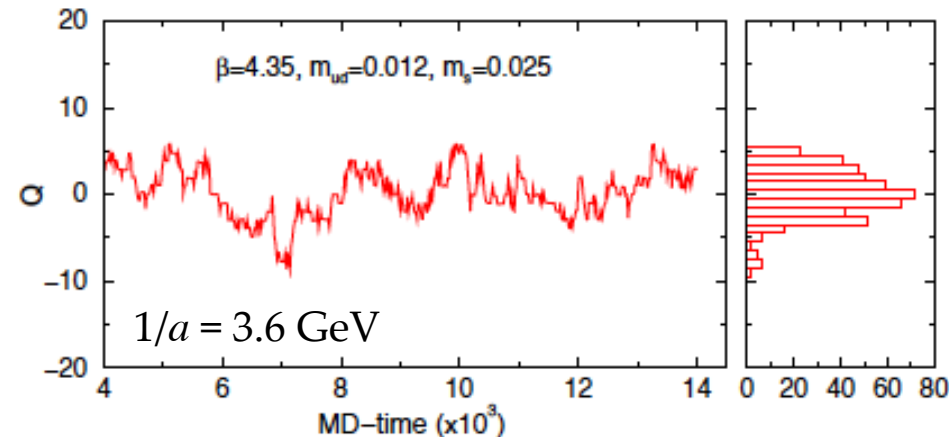
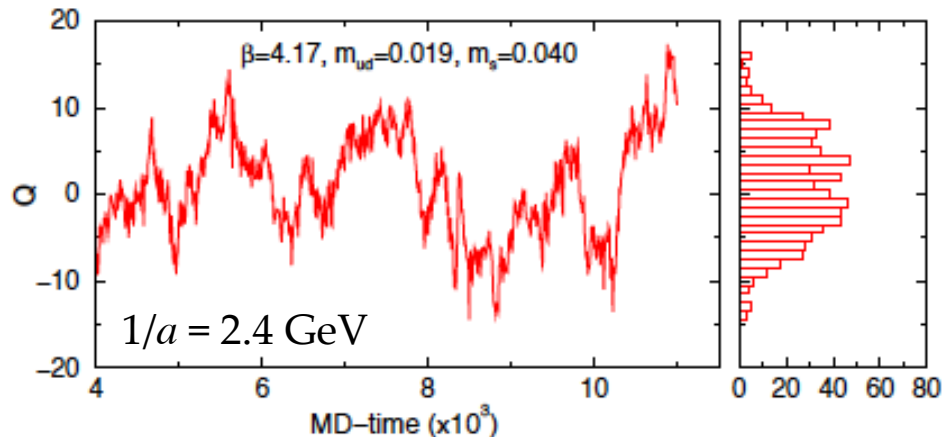


Topological charge

- Ensemble generation has been done. Test with basic quantities on-going: topological charge, lattice spacing, Ω baryon mass...

topological charge sampling:

Noaki et al. @ Lattice 2014

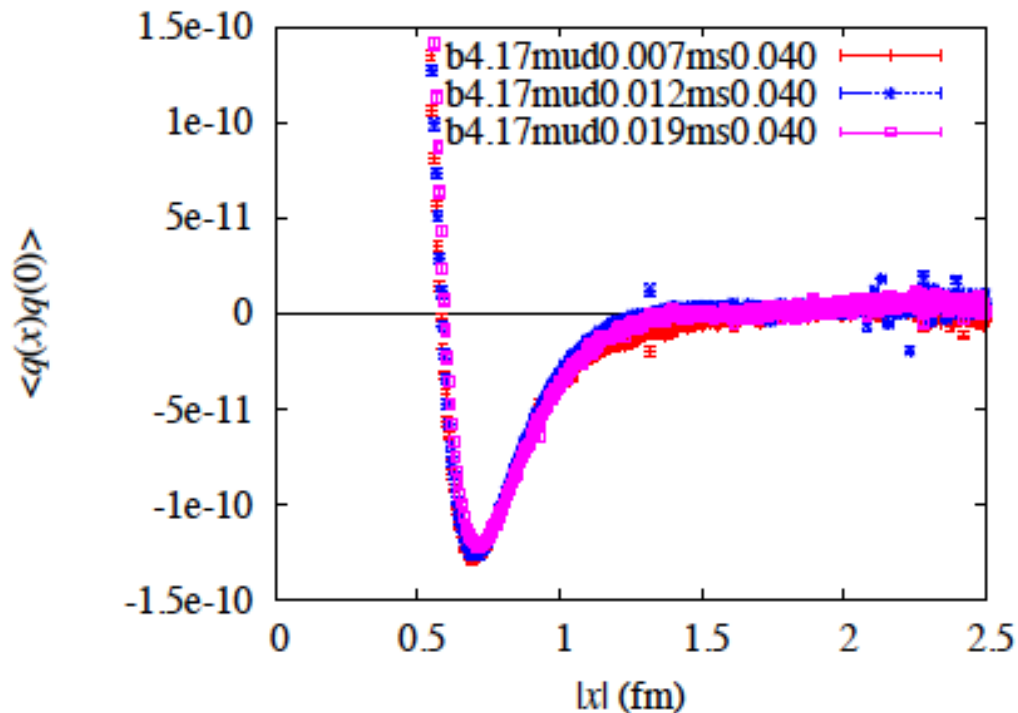


- Autocorrelation is long, but topological charge is changing.



Topological susceptibility

- $\chi_t = \langle Q^2 \rangle / V$, a measure of the local topological fluctuation
 - Can be evaluated from sub-volume topology, or equivalently from topological charge correlator.



$$\chi_t = \int d^4x \langle q(x)q(0) \rangle$$

Fukaya et al., 1411.1473

Topological charge density correlator calculated after a Wilson-flow.

- UV divergence $\sim 1/a^6$ at short distances.
- Cancelled by a pocket at the mid distances.



Topological susceptibility

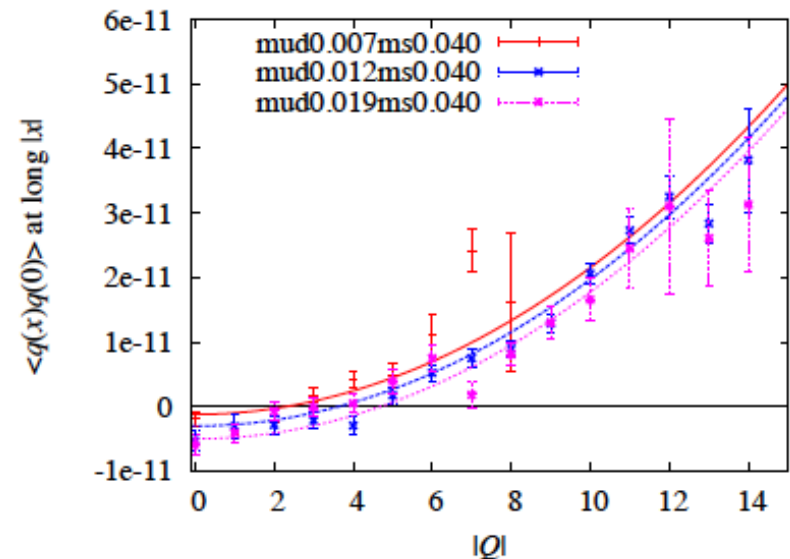
- $\chi_t = \langle Q^2 \rangle / V$, a measure of the local topological fluctuation
 - Can be measured locally.

$$\chi_t = \int_{|x| < r_{cut}} d^4 x \langle q(x) q(0) \rangle + O(e^{-m_\eta |x|})$$

- Eliminate the bias due to (slowly-moving) global topology using the relation

$$\langle q(x) q(0) \rangle_Q \sim \frac{1}{V} \left[\frac{Q^2}{V} - \chi_t \right]$$

at long distances

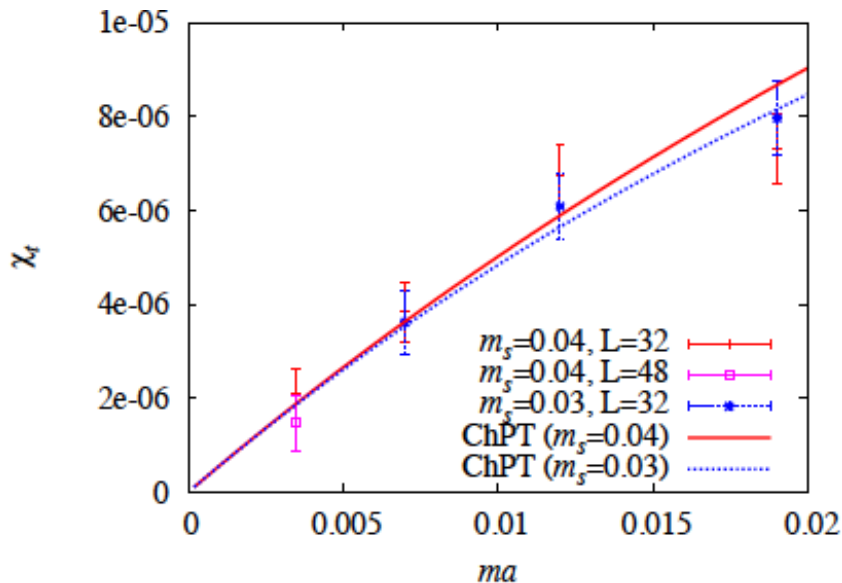


Topological susceptibility

- $\chi_t = \langle Q^2 \rangle / V$, a measure of the local topological fluctuation
 - Subtract the bias as

$$\bar{\chi}_t = \frac{V}{V - V_{sub}} \left\langle \int_{|x| < r_{cut}} d^4x q(x)q(0) - \frac{V_{sub}}{V^2} Q^2 \right\rangle$$

- Results show a suppression due to dynamical quarks:



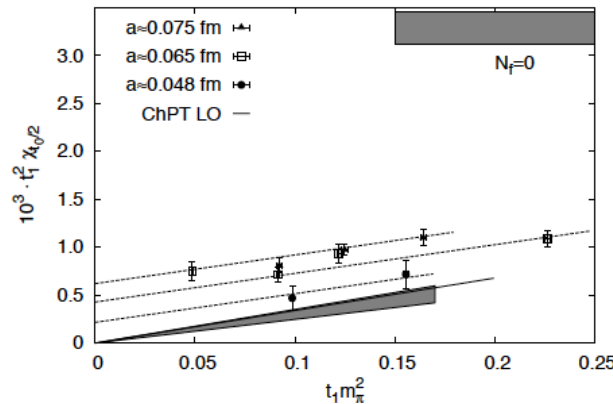
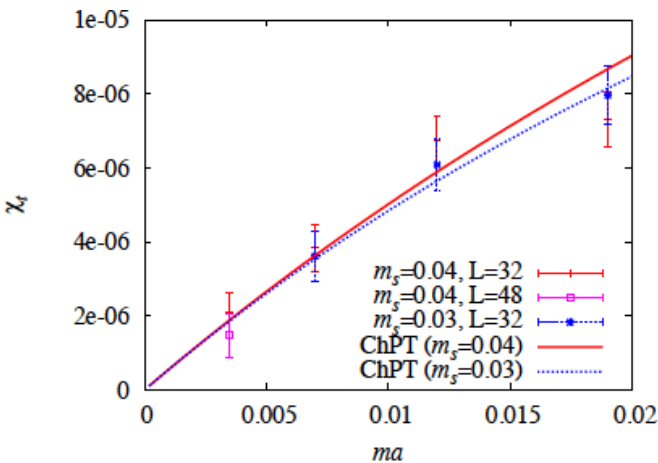
$$\chi_t^{\text{ChPT}} = \frac{\Sigma}{1/m_u + 1/m_d + 1/m_s}$$



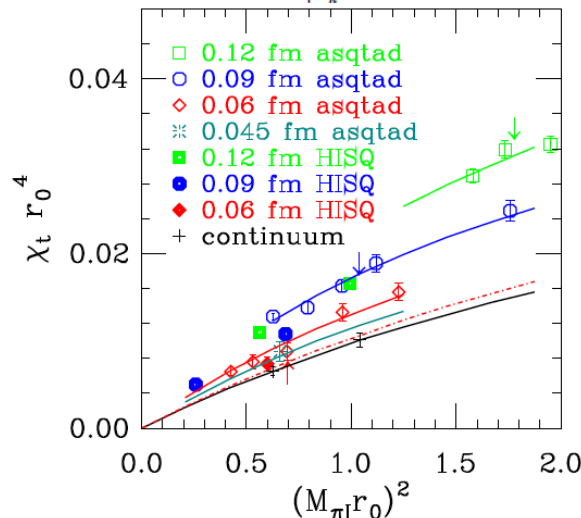
Topological susceptibility

- Key property to characterize the QCD vacuum. Well reproduced with chiral symmetry

$$\chi_t^{\text{ChPT}} = \frac{\Sigma}{1/m_u + 1/m_d + 1/m_s}$$



Wilson fermion:
ALPHA, arXiv:1406.5363.



Staggered fermion:
MILC, arXiv:1212.4768.



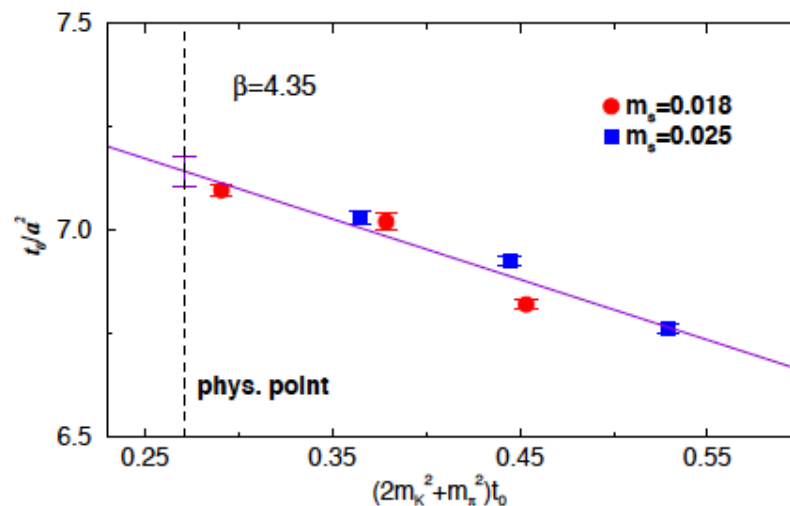
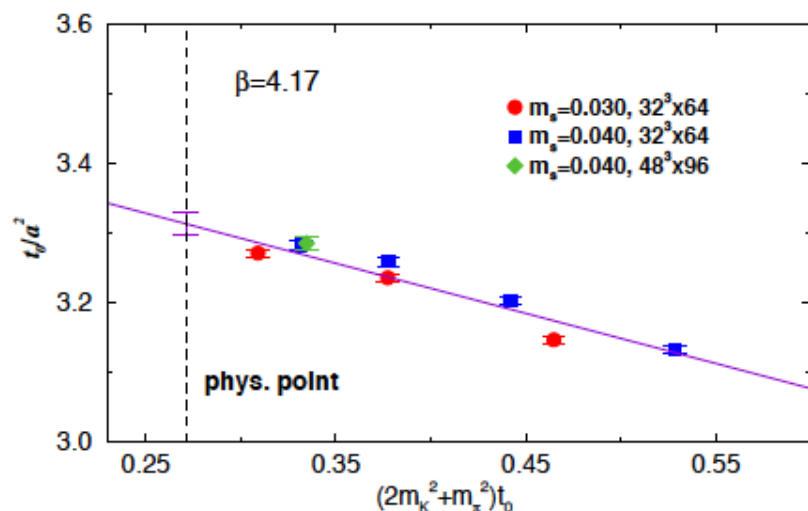
Scale setting

- Scale setting using the Wilson flow

$$t^2 \langle E \rangle \Big|_{t=t_0} = 0.3$$

- Energy density $\langle E \rangle$ after a Wilson flow (Luscher, 2010)
- Quark mass dependence consistent with previous works (Sommer, 2013)

Noaki et al. @ Lattice 2014



Mass dependence consistent with Sommer et al. (2013)

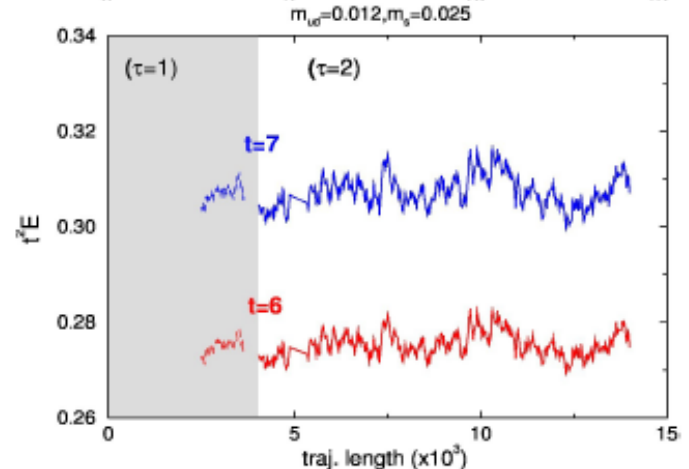
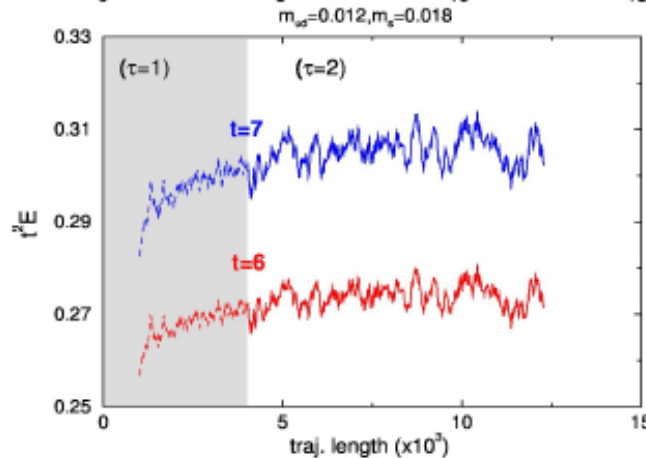
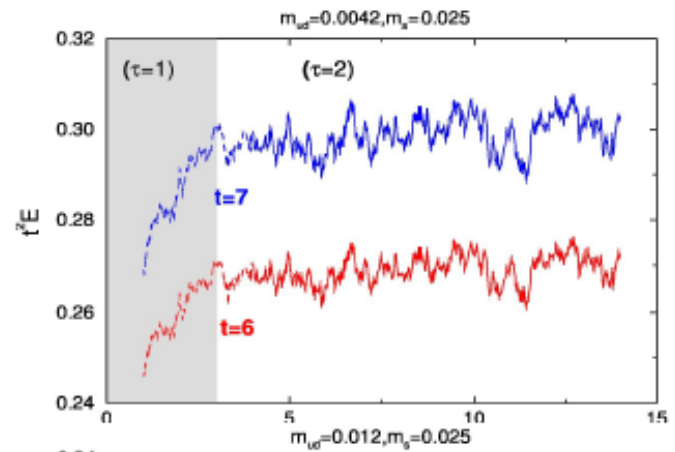
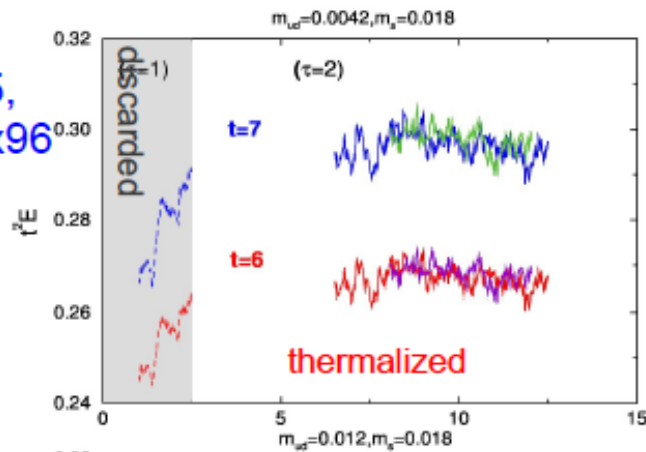


Scale setting

- Need to be careful about thermalization

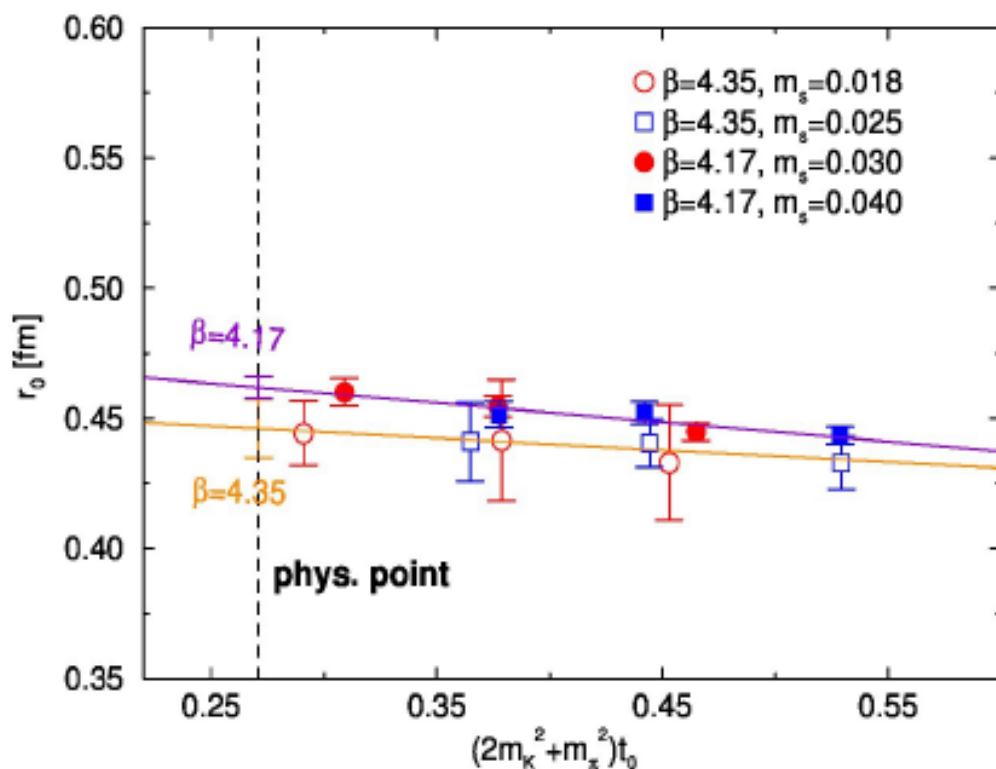
▶ history of $t^2 \langle E \rangle$ (around t_0) JLQCD, 2013

$\beta = 4.35,$
 $48^3 \times 96$



Scale setting

- Consistency with r_0 (from quark potential)



$\beta = 4.17: \quad r_0 = 0.462(4) \text{ fm}$

$\beta = 4.35$ (very preliminary):

$r_0 = 0.45(1) \text{ fm}$

cf. $r_0 = 0.465 \text{ fm}$ frequently used

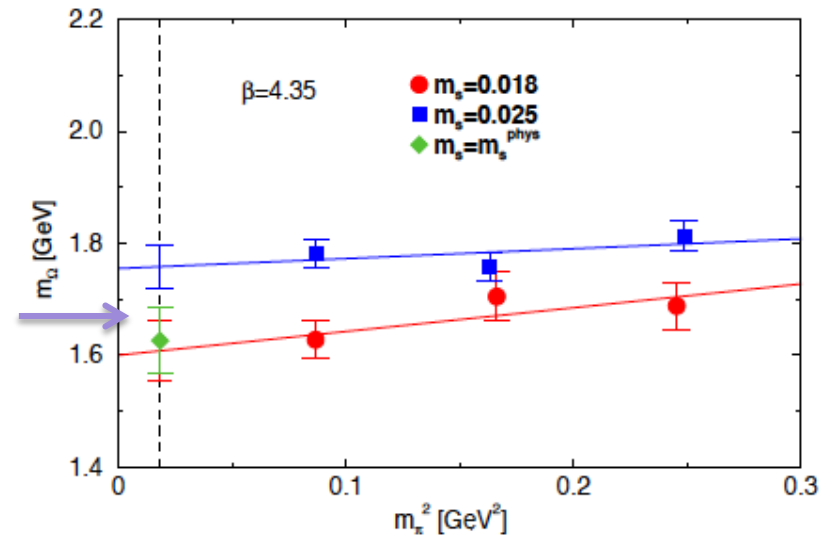
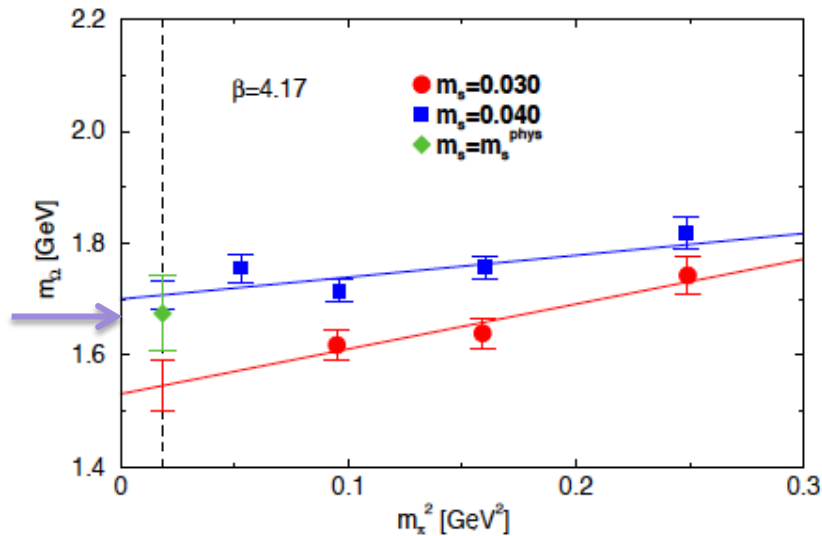
by , e.g. MILC Collab.



Ω^- baryon mass

- Baryon of (sss)
 - no chiral extrapolation needed, in the valence sector.
 - interpolation with two different strange quark masses.
 - consistent with exp data.

Noaki et al. @ Lattice 2014



3. First physics results

Short distance current correlator

Meson decay constants



Targeting applications

- Particle phenomenology
 - Form factors needed in the SuperKEKB experiment
 - Leptonic: $D \rightarrow l\nu$, $B \rightarrow l\nu$, also light mesons
 - Semi-leptonic: $B \rightarrow D^{(*)}l\nu$, $B \rightarrow \pi l\nu$, etc
 - Muon $g-2$
 - Vacuum polarization function (How much can we approach the experimental precision?)
 - Hadronic light-by-light (starting from the $\pi^0 \rightarrow \gamma\gamma$ amplitude)
- Others
 - Short-distance correlators (also for operator renormalization)
 - Vacuum structure of QCD
 - Finite temperature phase transition (as a related, but a separate project)



Two-point correlators

In perturbation theory (at $m=0$)

$$\langle S(x)S(0) \rangle = \langle P(x)P(0) \rangle = \frac{N_c}{\pi^4 (x^2)^3} \left\{ 1 + 2 \frac{\alpha_s}{4\pi} \left(\frac{4}{\epsilon'} - \frac{\gamma_S^{(0)}}{2} \ln \left(\frac{\mu^2 x^2}{4} \right) \right) + \dots \right\}$$

$$\langle V_\mu(x)V_\nu(0) \rangle = \langle A_\mu(x)A_\nu(0) \rangle = -\frac{2N_c}{\pi^4 (x^2)^3} \left(\frac{1}{2} \delta_{\mu\nu} - \frac{x_\mu x_\nu}{x^2} \right) \left\{ 1 + 4 \frac{\alpha_s}{4\pi} + \dots \right\}$$

- Both behave as $1/x^6$ at short distances.
- Extra divergence for $\langle SS \rangle$ and $\langle PP \rangle$ from the S and P operators. Once they are renormalized, correlators are finite at non-zero distances
- $\langle VV \rangle$ and $\langle AA \rangle$ are finite at non-zero distances.



Operator renormalization

In other words, they can be used to renormalize the lattice operators

$$Z_{\Gamma}^{\overline{MS}/lat}(\mu a) O_{\Gamma}^{lat}(a) = O_{\Gamma}^{\overline{MS}}(\mu)$$

- Renormalization condition = reproduce the MSbar result at a finite distance x .

Martinelli et al., PLB411, 141 (1997).

$$\Pi_{PP}(x) = \langle P(x)P(0) \rangle, \quad \Pi_{SS}(x) = \langle S(x)S(0) \rangle,$$

$$\Pi_{VV}(x) = \sum_{\mu=1}^4 \langle V_{\mu}(x)V_{\mu}(0) \rangle, \quad \Pi_{AA}(x) = \sum_{\mu=1}^4 \langle A_{\mu}(x)A_{\mu}(0) \rangle$$

$$\left[Z_{\Gamma}^{\overline{MS}/lat}(\mu a) \right]^2 \Pi_{\Gamma\Gamma}^{lat}(x) = \Pi_{\Gamma\Gamma}^{\overline{MS}}(x, \mu) \quad \text{or} \quad Z_{\Gamma}^{\overline{MS}/lat}(\mu a) = \sqrt{\frac{\Pi_{\Gamma\Gamma}^{\overline{MS}}(x, \mu)}{\Pi_{\Gamma\Gamma}^{lat}(x)}}$$



Operator renormalization

Necessary condition = result must be x -independent

$$Z_{\Gamma}^{\overline{MS}/lat}(\mu a) = \sqrt{\frac{\Pi_{\Gamma}^{\overline{MS}}(x, \mu)}{\Pi_{\Gamma}^{lat}(x)}}$$

1. Distance x must be small so that perturbative expansion converges.
2. Distance x must be large so that discretization effect is under control.

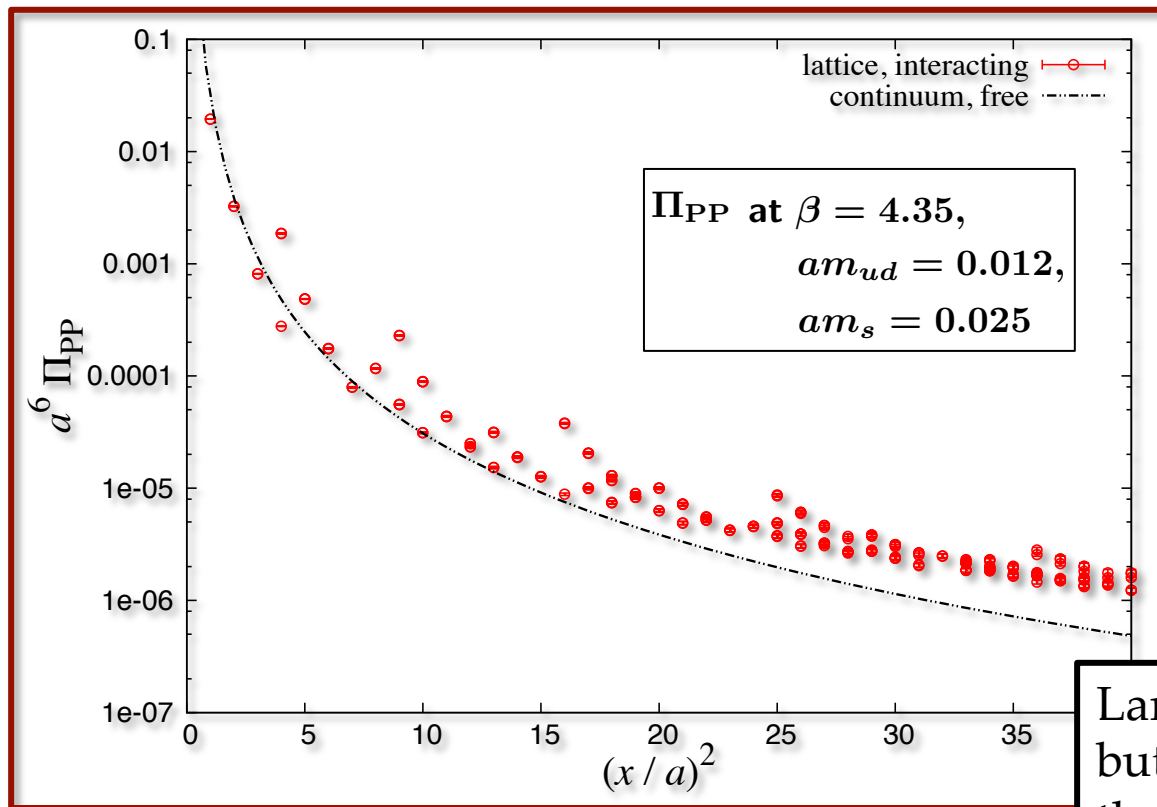
→ Need to find a window: $a \ll x \ll \Lambda_{\text{QCD}}^{-1}$

In other words, $\Pi_{\Gamma}^{lat}(x) \propto \Pi_{\Gamma}^{\overline{MS}}(x, \mu)$ has to be checked.



First look

- Two-point correlator as calculated on the lattice:



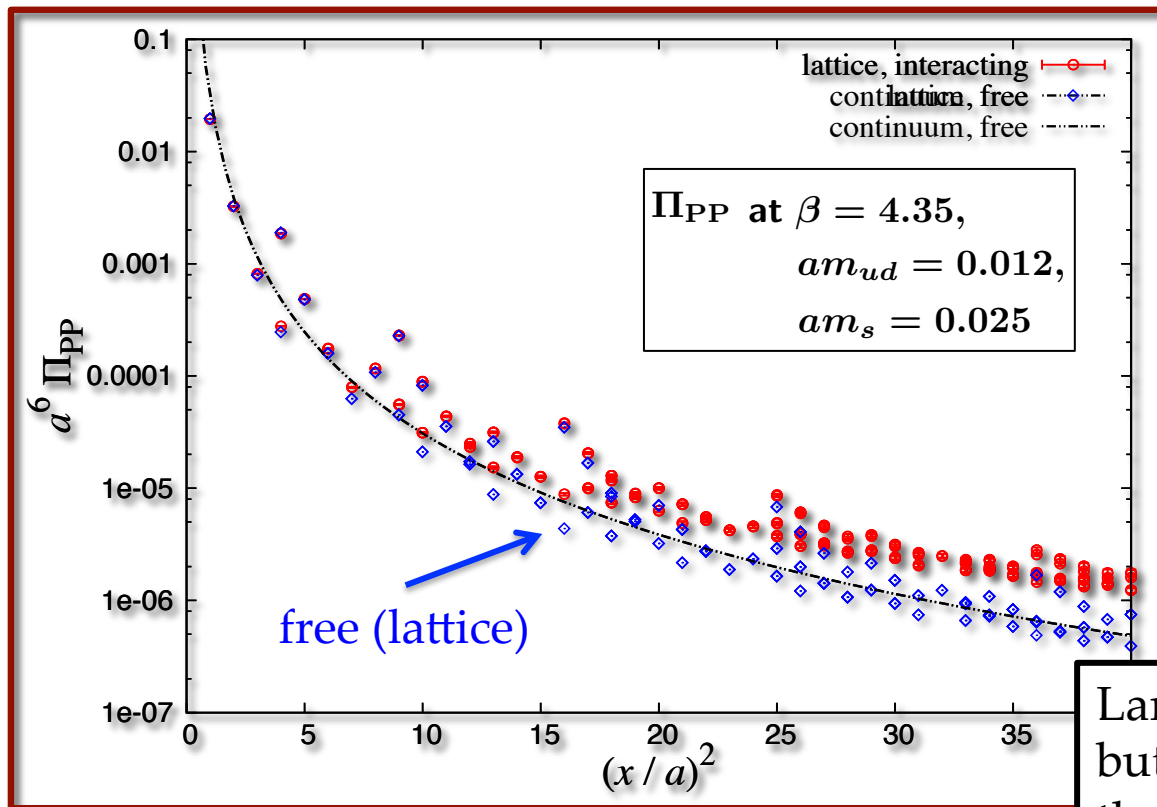
From Tomii @
Lattice 2014

Large disc effect is visible,
but very similar to that in
the non-interacting case.



First look

- Two-point correlator as calculated on the lattice:



From Tomii @
Lattice 2014

Large disc effect is visible,
but very similar to that in
the non-interacting case.



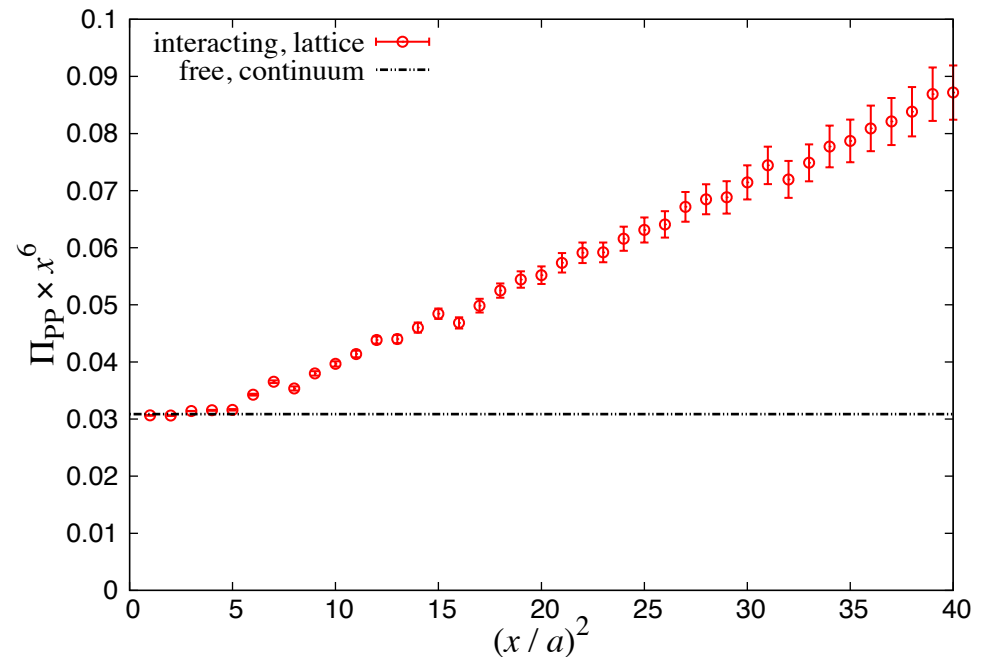
Eliminating the leading effect

- By subtracting the discretization effect calculated at the tree level,

$$\begin{aligned}\Pi_{\Gamma\Gamma}^{lat}(x) &\rightarrow \Pi'_{\Gamma\Gamma}{}^{lat}(x) \\ &= \Pi_{\Gamma\Gamma}^{lat}(x) + \Pi_{\Gamma\Gamma}^{cont,free}(x) \\ &\quad - \Pi_{\Gamma\Gamma}^{lat,free}(x)\end{aligned}$$

The bulk of the disc effect is eliminated.

See also, Gimenez et al., PLB598, 227 (2004), in which the correction is done multiplicatively.

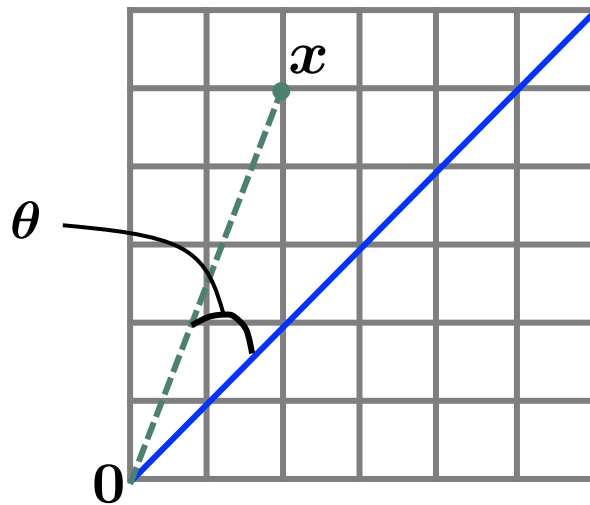


Filtering the points

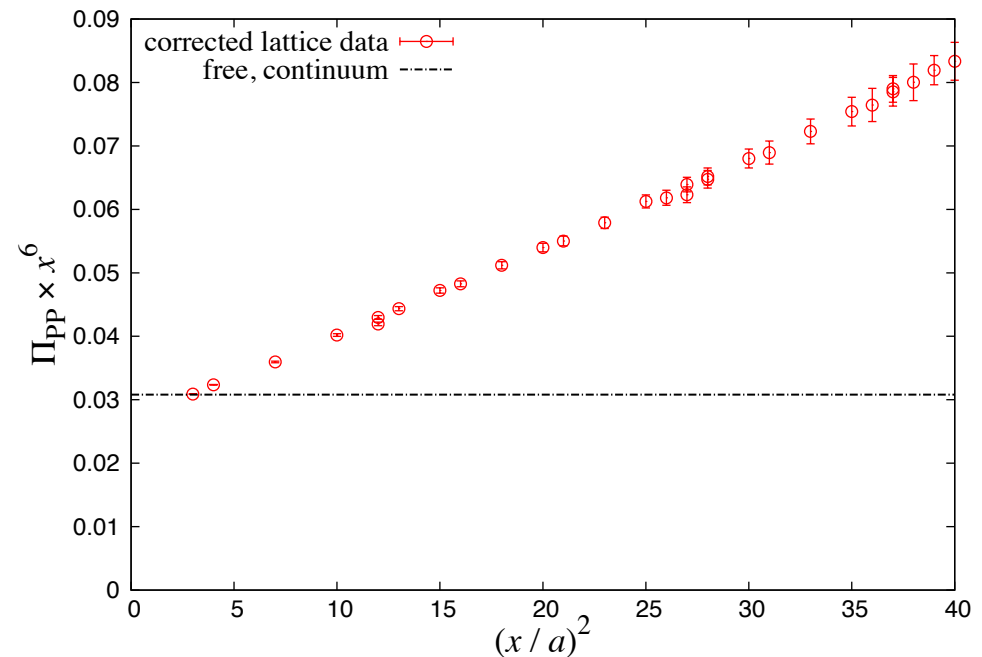
- Disc error is larger on the direction of lattice coordinates. Filter them out.

Further reduction of the disc effects.

Cichy et al., NPB865, 268 (2012).



Cut the points of $\theta > 30^\circ$
(angle from $(1,1,1)$).



Perturbative expansion

- Available to $O(\alpha_s^4)$. Chetyrkin, Maier, NPB844, 266 (2011).

$$\Pi_{\text{PP,SS}}^{\overline{\text{MS}}}(x, \mu) = \Pi_{\text{PP,SS}}^{\widetilde{\text{MS}}}(x, \tilde{\mu}) = \frac{3}{\pi^4 x^6} \left(1 + \sum_{n=1}^{\infty} \tilde{C}_n^{\text{S}} \tilde{a}_s^n \right)$$

$$\Pi_{\text{VV,AA}}^{\overline{\text{MS}}}(x) = \Pi_{\text{VV,AA}}^{\widetilde{\text{MS}}}(x) = \frac{6}{\pi^4 x^6} \left(1 + \sum_{n=1}^{\infty} \tilde{C}_n^{\text{V}} \tilde{a}_s^n \right)$$

$$\tilde{a}_s = \frac{\alpha_s^{\overline{\text{MS}}}(\tilde{\mu} = 1/x)}{\pi} = \frac{\alpha_s^{\overline{\text{MS}}}(\mu = 2e^{-\gamma_E}/x)}{\pi} \quad \text{to simplify the analytic expression}$$

- Scale evolution to $\mu=2$ GeV.

$$\Pi_{\text{SS,PP}}^{\widetilde{\text{MS}}}(x, \tilde{\mu}') = \frac{c(a_s(\tilde{\mu}'))}{c(a_s(\tilde{\mu}))} \Pi_{\text{SS,PP}}^{\widetilde{\text{MS}}}(x, \tilde{\mu}) \quad \text{Also known to } O(\alpha_s^4).$$

$$\Pi_{\text{VV,AA}}^{\widetilde{\text{MS}}}(x) \quad \text{Scale independent}$$

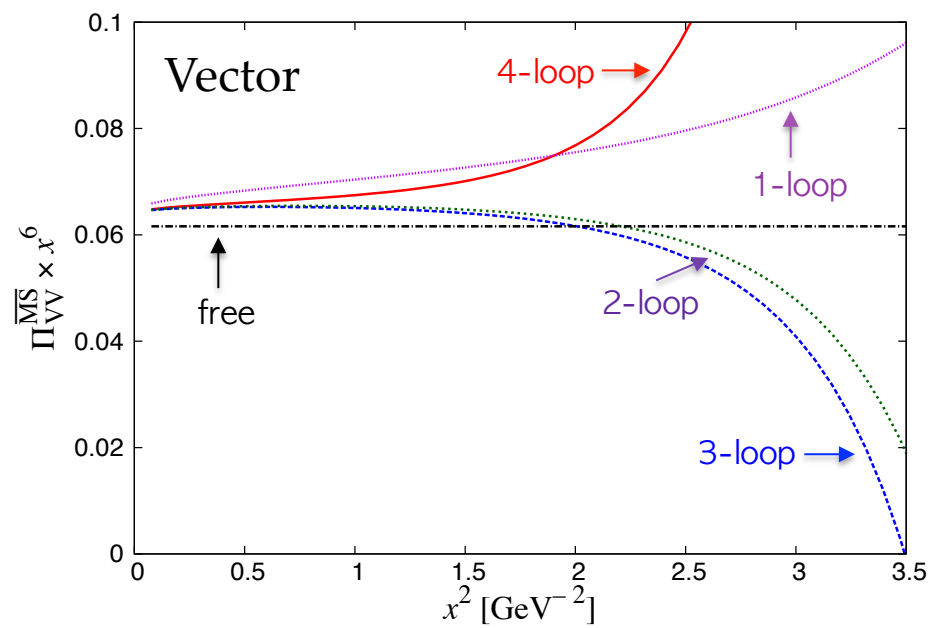
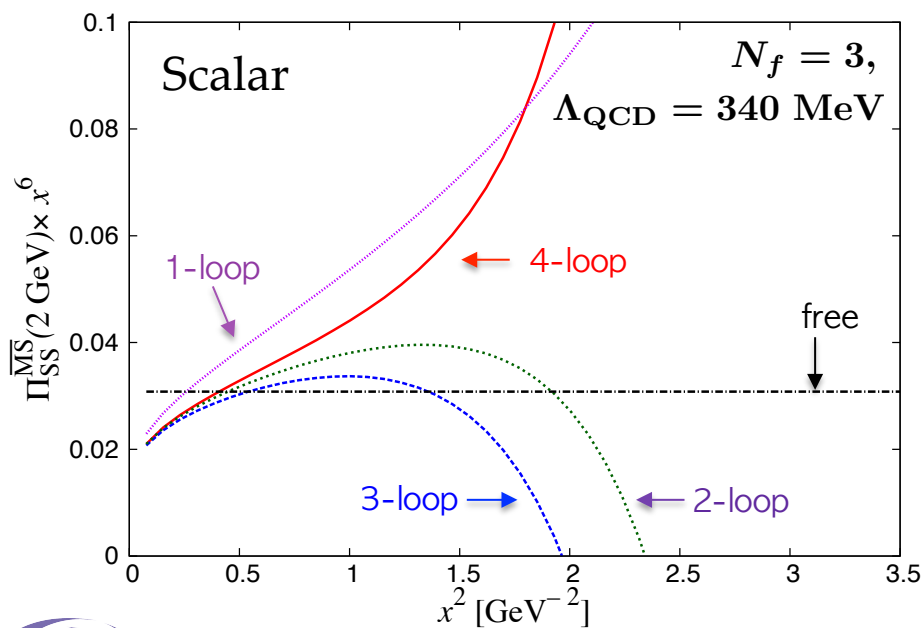


Perturbative expansion

- Bad convergence in the region of interest, if used as it is...

$$\Pi_{\text{SS}}^{\widetilde{\text{MS}}}(x, \tilde{\mu}) = \frac{3}{\pi^4 x^6} (1 + 0.67\tilde{a}_s - 16.3\tilde{a}_s^2 - 31\tilde{a}_s^3 + 497\tilde{a}_s^4)$$

$$\Pi_{\text{VV}}^{\widetilde{\text{MS}}}(x) = \frac{6}{\pi^4 x^6} (1 + \tilde{a}_s - 4\tilde{a}_s^2 - 1.9\tilde{a}_s^3 + 94\tilde{a}_s^4)$$



Better convergence

- With the BLM scale setting Brodsky, Lepage, Mackenzie, PRD28, 228 (1983).
 - Resum a class of diagram by choosing

$$\tilde{\mu}^* = \tilde{\mu} \exp(-11/6 + 2\zeta(3)) \simeq 1.8\tilde{\mu}$$
 and rearranging the perturbative expansion.

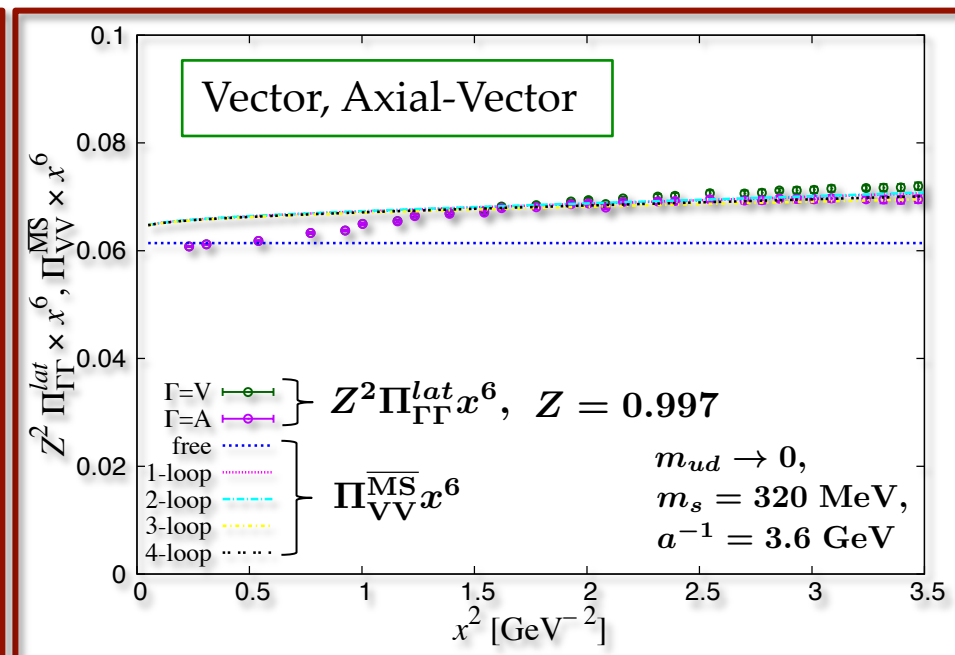
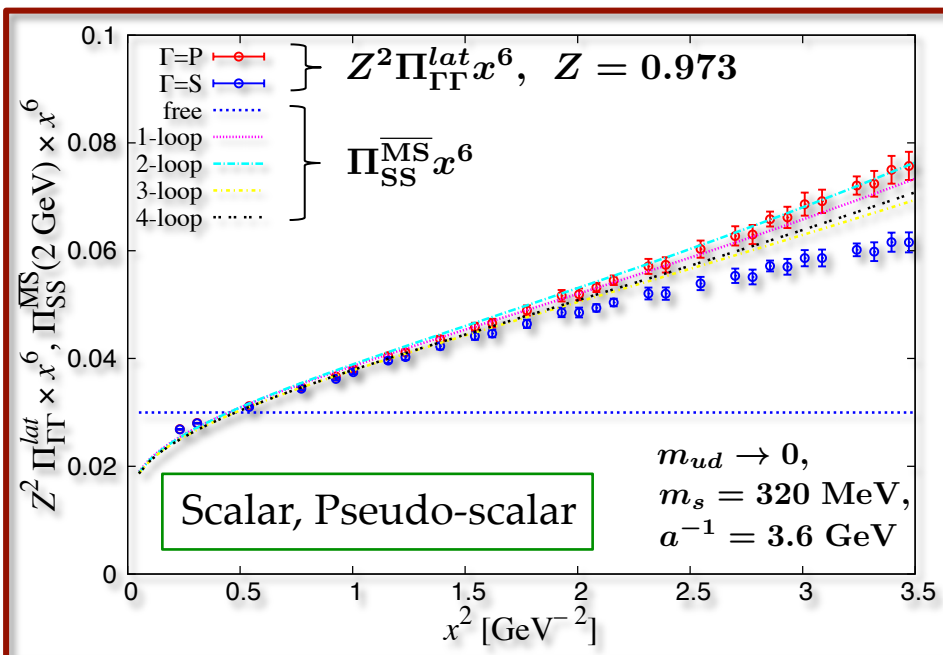
$$\left\{ \begin{array}{l} \Pi_{\text{SS}}^{\widetilde{\text{MS}}}(x, \tilde{\mu}) = \frac{3}{\pi^4 x^6} (1 + 0.67\tilde{a}_s - 16.3\tilde{a}_s^2 - 31\tilde{a}_s^3 + 497\tilde{a}_s^4) \\ \Pi_{\text{SS}}^{\widetilde{\text{MS}}}(x, \tilde{\mu}^*) = \frac{3}{\pi^4 x^6} (1 + 2.9\tilde{a}_s^* + 1.1\tilde{a}_s^{*2} - 42\tilde{a}_s^{*3} + 24\tilde{a}_s^{*4}) \end{array} \right.$$

$$\left\{ \begin{array}{l} \Pi_{\text{VV}}^{\widetilde{\text{MS}}}(x) = \frac{6}{\pi^4 x^6} (1 + \tilde{a}_s - 4\tilde{a}_s^2 - 1.9\tilde{a}_s^3 + 94\tilde{a}_s^4) \\ \Pi_{\text{VV}}^{\widetilde{\text{MS}}}(x) = \frac{6}{\pi^4 x^6} (1 + \tilde{a}_s^* + 0.083\tilde{a}_s^{*2} - 6\tilde{a}_s^{*3} + 18\tilde{a}_s^{*4}) \quad \tilde{a}_s^* = a_s(\tilde{\mu}^*) \end{array} \right.$$



Comparison

- Between the lattice and continuum
 - After taking the chiral limit (linearly in m) of the lattice data.

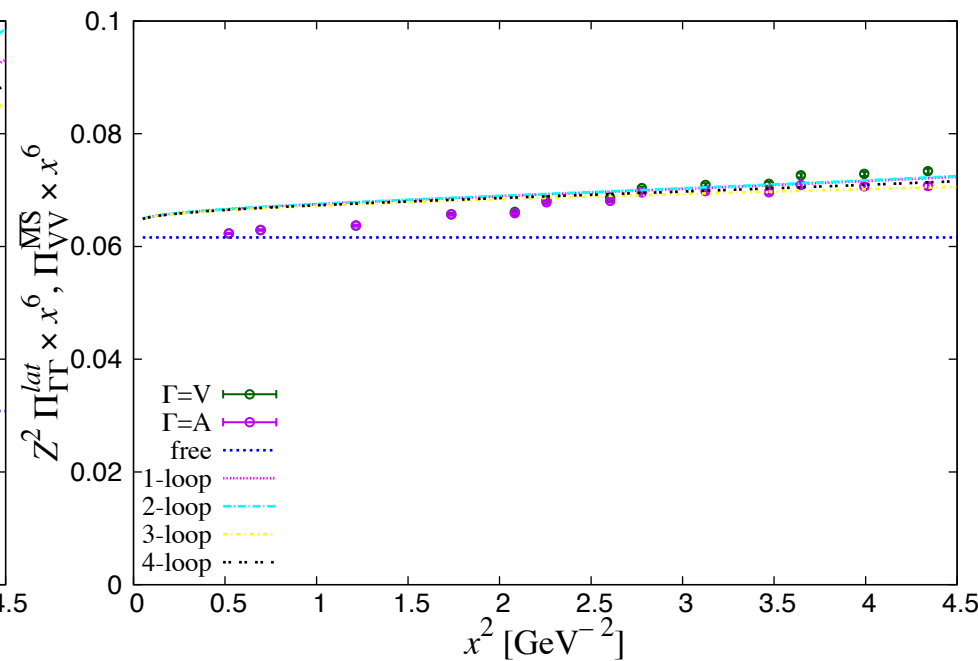
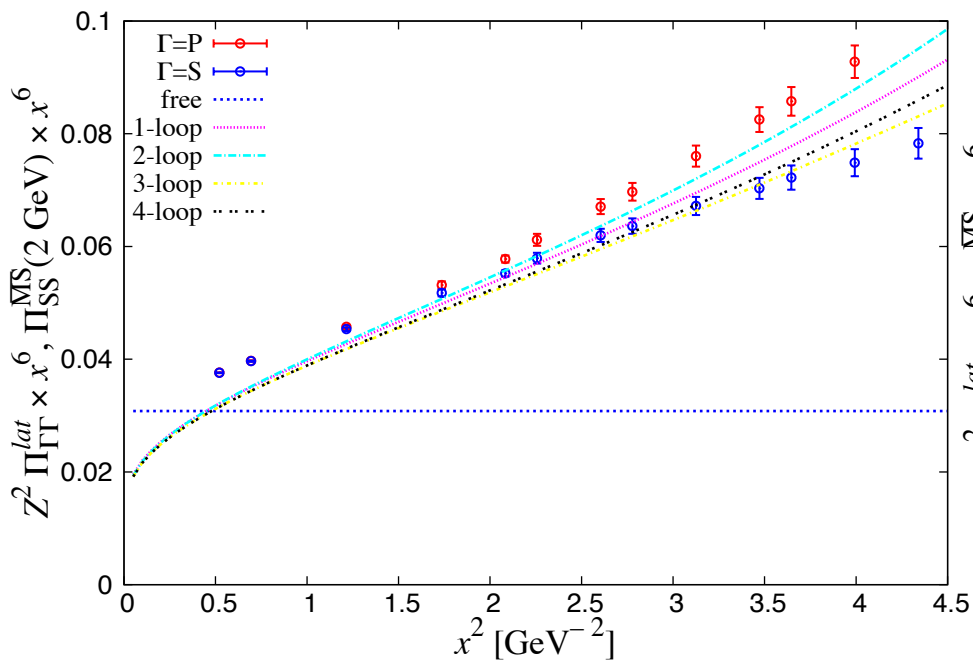


The Window can be identified.



Comparison

- Similar plots at a coarser lattice ($1/a = 2.4$ GeV)



Renormalization factor

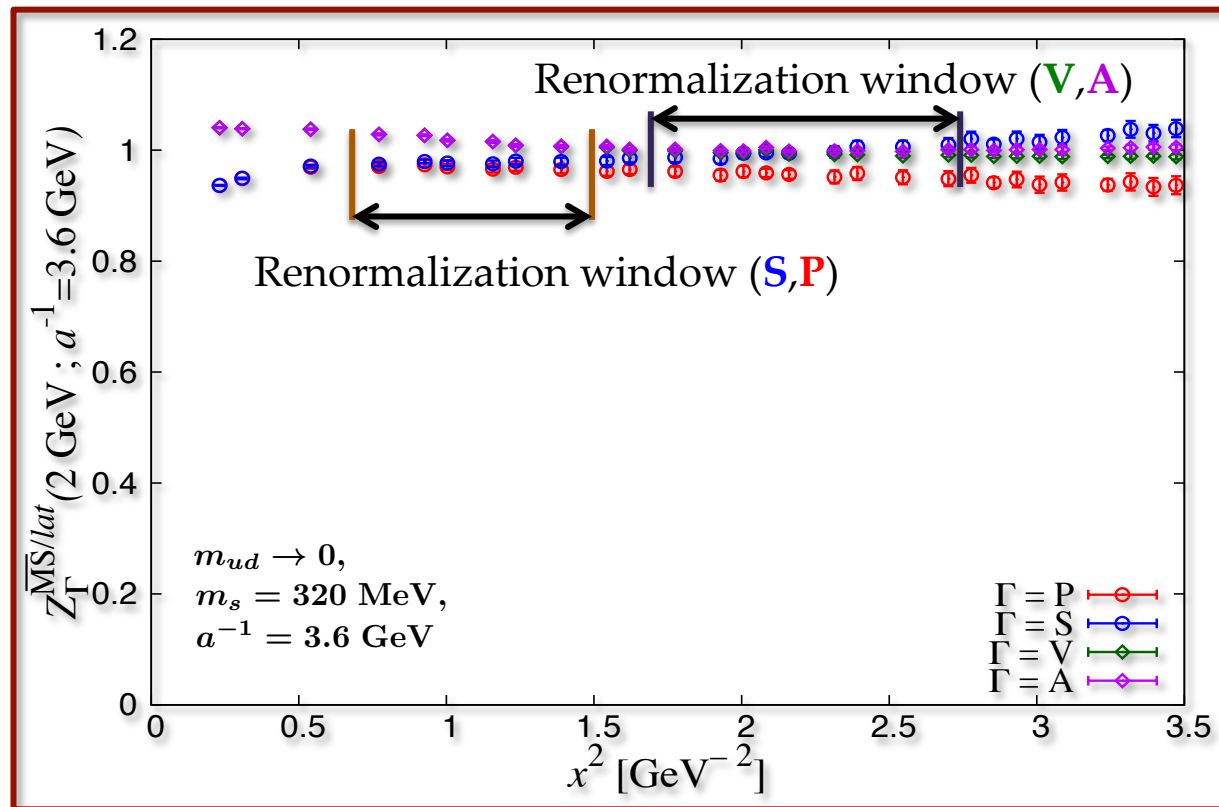
- Obtained from the ratio $Z_{\Gamma}^{\overline{\text{MS}}/lat}(2 \text{ GeV}) = \sqrt{\frac{\Pi_{\Gamma\Gamma}^{\overline{\text{MS}}}(x, 2 \text{ GeV})}{\Pi_{\Gamma\Gamma}^{lat}(x)}}$

At $\beta = 4.35$, $m_s = 0.0180$

$$Z_S^{\overline{\text{MS}}/lat}(2 \text{ GeV}) = 0.973 \pm 0.005 \pm 0.005$$

statistical
↓
↑
systematic

$$Z_V^{\overline{\text{MS}}/lat} = 0.997 \pm 0.003 \pm 0.004$$



Phenomenology

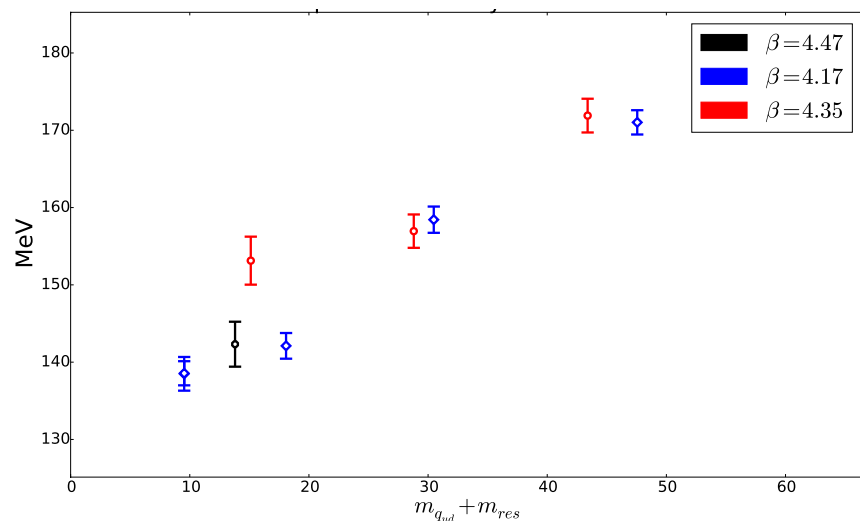
- Another example that the lattice data at short distances are well described by perturbation theory.
 - “Window” exists around $x \sim 1 \text{ GeV}^{-1}$.
 - Only after improving both lattice and continuum.
 - Remaining disc effect seems to be smaller than literal $O(a^2x^2)$.
- Applications
 - Precise calculation of renormalization constants (4-loop available on the continuum side).
 - Extracting α_s from the x dependence.
 - Test of the OPE expressions, extraction of the condensates appearing at higher orders.



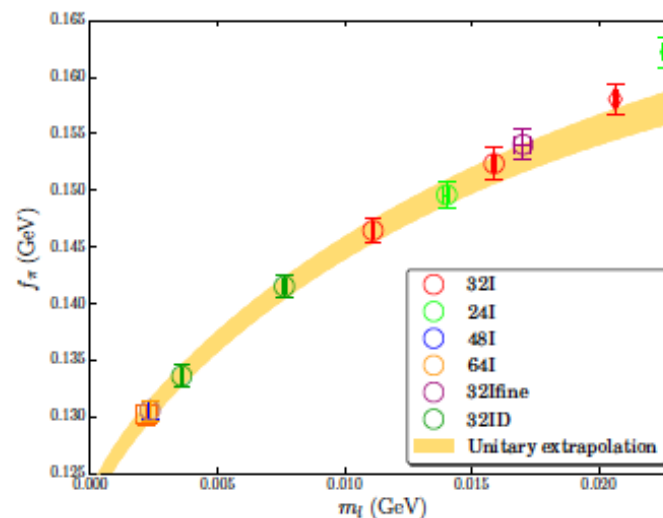
Decay constant

- More standard calculation:
 - 3 lattice spacings (all less than 0.1 fm)

f_π : Fahy et al. (very preliminary)



RBC/UKQCD, arXiv:1411.7017



Currently improving statistics...

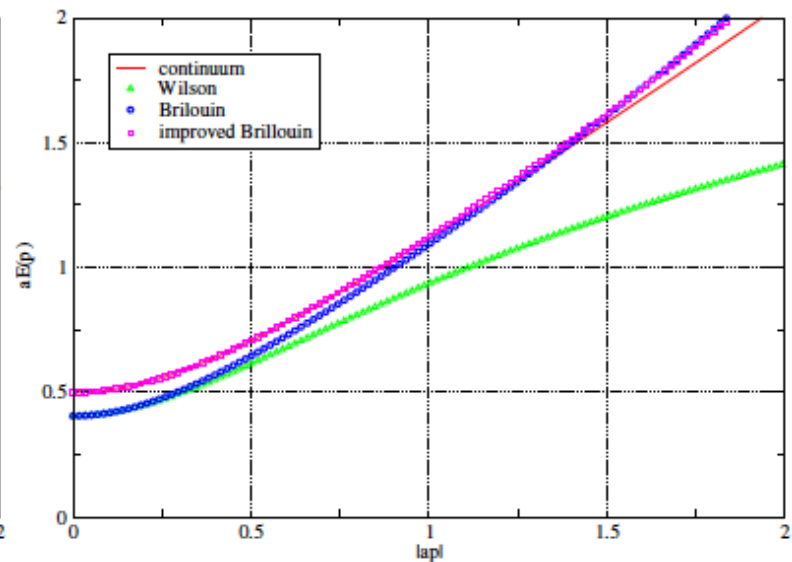
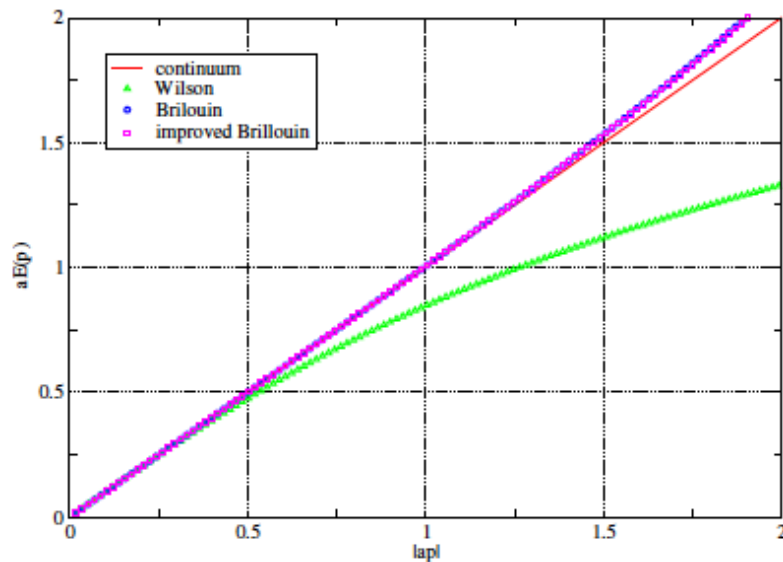


Heavy quarks

(Starting from charm, with Mobius domain-wall)

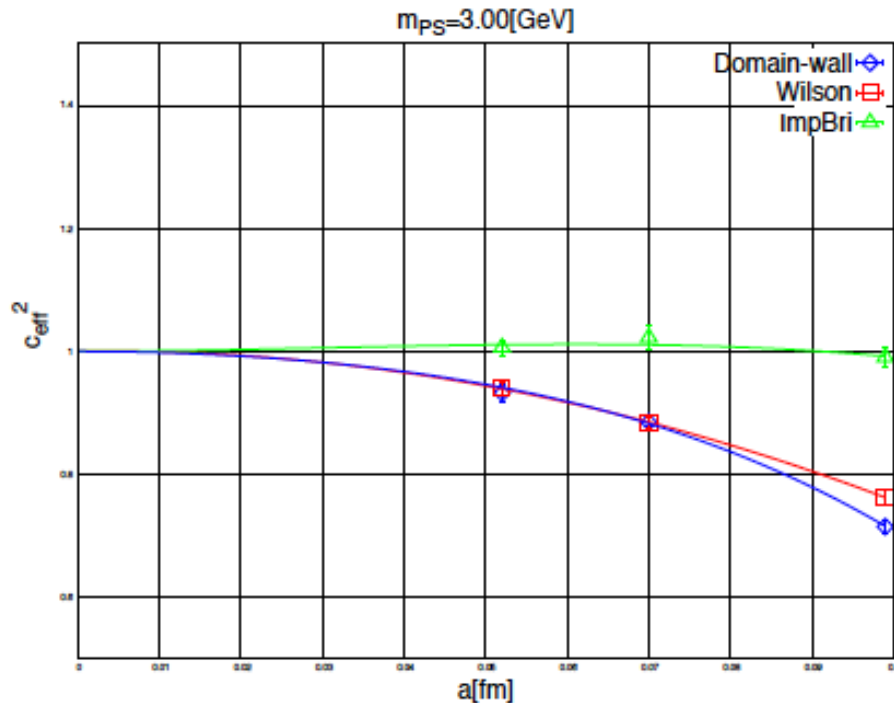
- Brillouin-type fermions
 - Excellent dispersion relation for heavy quarks

Cho et al. @ Lattice 2013, 2014



Brillouin-type fermions

- Non-perturbative test
 - Speed-of-light for charmonium
 - On quenched lattices



Cho et al. @ Lattice 2014

$$c_{eff}^2(p) = \frac{E(p) - E^2(0)}{p^2}$$

Promising formulation,
for future use.



Summary

- New generation of dynamical gauge configs appearing
 - With chiral lattice fermions
 - At small lattice spacings (down to 0.043 fm)
- Physics applications
 - Light hadron mass : bread-and-butter
 - Topology : chiral symmetry is crucial.
 - Short-distance correlator : chiral symmetry is helpful.
 - Form factors : fine lattices will be crucial.

